A REVIEW OF THE OCEANOGRAPHY OF THE CENTRAL PACIFIC OCEAN IN THE VICINITY OF THE LINE ISLANDS

By

Richard A. Barkley
Oceanographer
U. S. Bureau of Commercial Fisheries
Biological Laboratory
Honolulu, Hawaii

March 1962

A REVIEW OF THE OCEANOGRAPHY OF THE CENTRAL PACIFIC OCEAN IN THE VICINITY OF THE LINE ISLANDS

By

Richard A. Barkley
Oceanographer
U. S. Bureau of Commercial Fisheries
Biological Laboratory
Honolulu, Hawaii

INTRODUCTION

The Pacific Ocean contains slightly more than half of all the water in the world's oceans, and its fifty million square miles of area cover 35 percent of the Earth's surface. The position of the Line Islands near the center of this vast expanse of water makes these islands one of the most remote groups in terms of distance from continental land masses. This report presents a brief summary of oceanographic conditions in this remote region. It deals with the area between 10° South and 20° North latitude, extending from 150° West to 170° West longitude. This region of two million square miles contains the Line Islands group of Palmyra, Washington, Fanning, Christmas, Jarvis, Malden, and Starbuck islands, as well as Johnston Island in the northwest, Penrhyn Island to the south, and the island of Hawaii in the northeast. It is a tropical area dominated by the Trade Winds and the Doldrums and by a system of four major surface and near-surface ocean currents, the North and South Equatorial Currents, which flow westward, and the Countercurrent and Equatorial Undercurrent, which flow to the east.

The major portion of this review consists of charts and sections showing a summary of the oceanographic data for this region. An attempt has been made to make these figures the most complete and accurate yet available; all the original data and the final values shown on the figures have gone through a preliminary editing, and several areas have been gone over in detail. These latter "spot samples" indicate that very few machine and human errors remain in the finished diagrams, but not enough time has been available to insure that all values shown are as free as humanly possible from errors. The text is intended as a review of salient features, and will therefore be briefer than a complete discussion of the oceanography of the area would warrant. Additional information can be found in the figures, and more detailed treatment of certain features will be found in reference material such as Sverdrup, Johnson and Fleming's textbook, "The Oceans" (1942), Defant's "Physical Oceanography" (Volume 1) (1961), and in an outstanding collection of papers on the equatorial circulation of the Pacific Ocean in volume VI of Deep-Sea Research (1960). These and other sources of information consulted in the preparation of this review are listed in the bibliography.

The oceanographic station data on which this summary is based were collected by the Dana Expedition in 1928, the Carnegie Expedition in 1929, the Albatross Expedition in 1947, and from the Hugh M. Smith of the Bureau of Commercial Fisheries Laboratory in Honolulu during the period from 1949 to 1957. A preliminary analysis of the station data then available on punched cards for the area from 130° West to 180° longitude and from 20° South to 10° North latitude was performed late in 1961 as a test of automatic data processing techniques. The present summary is based upon this previous study, together with additional data from the Northern Hemisphere, so that the charts, sections, and analysis of conditions north of the Equator are based on all of the available data through 1960. It was not possible to bring the data for the Southern Hemisphere area up to date in the time available, so the values and conclusions for this area are based on slightly less than half of all the data collected in that area.

The plankton collections discussed herein were made from the Hugh M. Smith and the Charles H. Gilbert, also of the Honolulu Laboratory of the Bureau of Commercial Fisheries. The work of summarizing the data from these collections for this report was performed by Mr. Everet C. Jones of the Honolulu Laboratory.

The charts of surface current vectors and the review of the bathymetry of the Line Islands area were prepared by Mr. Robert P. Brown, also of the Honolulu Laboratory.

The time-series observations of sea surface temperature and salinity at Christmas and Johnston islands were collected for this Laboratory by cooperating observers on these islands. Without their assistance our understanding of conditions in this region would be very much more limited than it now is.

BATHYMETRY AND GEOLOGY

Figure 1 shows the bathymetry of the Line Islands region. This chart, reproduced from H.O. Chart Misc. 15-254-6, shows the depths with contour intervals of 500 fathoms. The most prominent feature of the submarine topography is the Northwest Christmas Island Ridge that extends from the Equator at 150° W. for almost a thousand miles due northwest, to 12° N., 166° W. This ridge is composed of submerged volcanic mountains, many of which have coral atolls upon their summits. Christmas, Fanning, Washington and Palmyra islands are such atolls. The locations, land areas, etc. of this chain of atolls are given in Table 1.

The submarine slopes to seaward of these atolls are quite steep. In some cases they were found to be of the order of 2,500 to 3,000 feet to the mile (Wentworth, 1931). The ocean floor surrounding the Line Islands varies in depth between 15,000 to 18,000 feet. The greatest depths are found to the northeast and southwest of the chain.

Table 1.--Location and some characteristics of the Line Islands and Johnston Island

Island	Latitude N.	Longitude W.	Length (naut. mi.)	Width	Land area (naut. mi.^{2})	Lagoon area (naut. mi.^{2})	Maximum lagoon depth (feet)
Christmas	01°51'	157°23'	35.0	24.0	250.0	107.0	15
Fanning	03°52'	159°19'	9.9	6.0	13.0	42.6	50
Washington	04°43'	160°24'	3.4	1.3	2.8	1.1	30
Palmyra	05°52'	162°06'	4.0	1.5	1.5	12.0	160
Johnston	16°45'	169°30'	0.5	0.1		1.1	30

In the northwest portion of Figure 1, a part of the Marcus-Necker Seamount Chain appears. This ridge is also referred to as the mid-Pacific Mountains. Like the Christmas Island Ridge it is made up of submarine volcanic mountains having steep slopes. However, the Marcus-Necker Ridge supports only one small, partially raised coral atoll, Johnston Island.

The island of Hawaii, with its steep submarine slopes and associated seamounts, can be found in the northeastern portion of Figure 1. This island is still volcanically active, the only such island in the huge Hawaiian Ridge, which stretches for a distance of 1,660 nautical miles northwest of Hawaii to beyond Kure Island

Although the presence of islands and near-surface seamounts can be expected to modify the surface currents and water properties nearby, the islands in the area of interest are so small and scattered that their influence on the ocean must be quite minor, except in the case of Hawaii and the Hawaiian chain. In this latter case, there is evidence to suggest that the Hawaiian Ridge modifies the currents in a very large area of the North Pacific, generally deflecting the water toward the north on the upstream side and leaving a wake effect in the form of vortices of major dimensions downstream. These vortices or eddies, with diameters of the order of 50 to 100 miles, are frequently evident in oceanographic data taken to the west and southwest of Hawaii, but their behavior and effect on the general circulation have not been adequately investigated.

CLIMATOLOGY

The northern portion of the Line Islands area is located in the Northeast Trade Wind zone virtually the entire year, and the southern sections are located in the zone of the Southeast Trades. Between the Trade Wind zones lies an atmospheric low-pressure trough associated with rising warm moist air and characterized by winds which are weaker and more variable than those in the Trade Wind zones; this zone, called the Doldrums, marks the climatic Equator. In July the low-pressure trough is found in latitudes of about 5° N. to about 9° N.; in January, the trough is farther south, lying near 5° N. at 150° W., at about 0° near 160° W., and close to 5° S. at 170° W. (Riehl, 1954). Winds in the Trade Wind zone between 10° and 20° N. average 12 or more

knots in January-February and are within 45° of the mean direction 80 percent of the time. In the southwest portion of the Line Islands area, the January-February Trade Winds blow at speeds of 8 knots or less, on the average, and their direction is less constant. The wind velocity in the Trades is lower in July-August, with averages not exceeding 8 knots in most of the area of interest, except in the northeast, where average speeds of 12 knots or more are found. In general the mid-Pacific Trades are very constant in direction, being within 45° of the mean direction about 70 percent of the time (Riehl, 1954).

The pattern of precipitation is governed largely by the location and strength of the Doldrum low-pressure trough. For the oceans as a whole there is a maximum in the latitudinal distribution of rainfall at 5°-10° N., with average values of 187 centimeters of rainfall per year, compared to 96 cm./yr. for the average rainfall at all latitudes. As a result there is an excess of precipitation over evaporation of 61 cm./yr. in latitudes 5°-10° N., as compared to an ocean-wide deficit of precipitation over evaporation of 10.2 cm./yr. (Wuest, 1954). In the Line Islands region the rainfall in the Doldrums is greater than the world average, reaching 300 cm./yr. or more near 5° N., 170° W., and over 250 cm./yr. at 5° N., 150° W. The region of least rainfall is at 20° N., with about 60 cm./yr. at 150° W. and some 80 cm./yr. at 170° W. In the southern sections, there is a minimum of rainfall to the east, near latitude 5° S., with values of about 75 cm./yr. at 150° W. (Riehl, 1954). At Christmas Island the rainfall is highly variable, but the average rainfall is less than 3 cm. per month from August through February; most of the rain falls during March, April, and May, with a mean maximum of about 20 cm. in April.

Rainfall exceeds evaporation only in the narrow belt between 1° N. and 10° N. Elsewhere there is an excess of evaporation, with maxima at about 24° N. and 20° S. As a result of this, and of the currents, there is a minimum in the latitudinal distribution of surface salinity near 10° N., with salinity at the surface increasing both to the north and south of that latitude.

CURRENTS

The ocean currents at the surface in the Line Islands region are shown as vectors on Figure 2 through 6, which summarize the observed drift of vessels during the months of March through July. These charts were derived from H.O. Publications 596 and 570 (U.S. Navy Hydrographic Office, 1947 and 1950), which show the same information in different form. Each arrow on the charts represents a vector giving the mean velocity and direction of currents in the square surrounding the base of the arrow. The width of each arrow indicates the number of observations it represents. It should be mentioned that such data include the combined effects of the major ocean currents and the surface wind drift as well as the motion caused by drag of the wind on the vessels making the observations.

On Figure 2, the chart for March, the surface currents north of 8° N. and south of 5° N. show predominantly westward and northwestward flow, at speeds of 10 to 15 miles per day, with some values as high as 20 miles per day. In between these areas there are a number of indications of a narrow band of eastward flow, the Equatorial Countercurrent, with velocities on the whole of less than 10 miles per day. On the April chart, Figure 3, there is almost no trace of the Countercurrent at the surface. The flow is westerly with some northward component, at speeds of about 10 miles per day in the north, and up to 20 miles per day near the Equator. Conditions in May resemble those in March, with only a very few areas showing indications of the Countercurrent. By June (Figure 5) conditions have changed, with easterly flow present near 5° N. to the west of the chart, and near 6°-7° N. in the east. Velocities of 15 to 20 miles per day are less common than formerly, in the westerly Equatorial Currents, but higher velocities are found in the region of the Countercurrent. By July (Figure 6) the Countercurrent is well developed at the surface between 5° N. and 9° N. Velocities of over 15 miles per day with eastward components are common, with one value of 34 miles per day near 150° W. The westward flow near Christmas Island is more intense, with speeds of about 20 miles per day. In the northwest, near Johnston Island, more moderate velocities of about 10 miles per day, generally northwesterly, are found. These figures summarize the current observations for the surface layers during the early part of the year. The H.O. charts for other months show that currents in August, September and October are similar to those in July; the Countercurrent diminishes slightly in intensity as the year progresses, with the other currents remaining relatively steady. By January and February the Countercurrent appears quite weak; there is perhaps a slight intensification of the South Equatorial Current at this time.

An interesting case of long-distance transport of volcanic pumice through the Line Islands region is given by Richards (1958). An average speed of about 22 cm./sec. (0.43 knots) was calculated for the rate of transport from islands near Mexico to Hawaii, Johnston Island and the Marshalls.

Subsurface current velocities can be computed as geostrophic currents, that is, currents in which the horizontal pressure gradients are in balance with Coriolis' force so that the current flow is parallel to the isobars. Both theory and practice indicate that currents in mid-ocean are essentially geostrophic, except at the Equator, where Coriolis' force vanishes, and at the surface where wind stress must also be considered in the balance of forces governing water movement. A discussion of the theory and computation of geostrophic currents can be found in Sverdrup et al. (1942).

Figure 7 and Table 2 can be used to compute the geostrophic currents in two north-south sections in the Line Islands region. To determine the current at a given latitude and depth, the slope of the line in Figure 7 for the appropriate depth level (0, 50, 100,... 700

decibars, which can be taken with sufficient accuracy to be equivalent to depths in meters) shown in the middle of the graph is determined at the desired latitude, in units of dynamic centimeters per degree of latitude (1 dynamic meter = 100 dynamic centimeters). Multiplying this slope by the velocity figure for the proper latitude in Table 2 gives the desired east-west velocity. Thus, in Figure 7, at a depth of 150 meters at 8° N. between 150° W. and 160° W., the slope is 0.80 dynamic meters per 30° of latitude, or 2.7 dynamic centimeters per degree of latitude. Multiplying this value by the velocity shown in Table 2, for a slope of one dynamic centimeter per degree at 8° N., of 4.4 cm./sec. or 0.086 knots, gives a computed current velocity of 12 cm./sec. or 0.23 knots. The direction of flow can be determined using the rule in Table 2; since the dynamic height anomaly decreases toward the pole at 8° N., the current must have an eastward component.

Table 2.--Geostrophic current velocity as a function of latitude, for a gradient of 1 dynamic centimeter per degree of latitude

ϕ	U		ϕ	U	
Degrees	Cm./sec.	Knots	Degrees	Cm./sec.	Knots
1	52.0	1.0	11	3.2	0.062
2	18.0	0.35	12	3.0	0.058
3	12.0	0.23	13	2.8	0.054
4	8.8	0.17	14	2.6	0.051
5	7.1	0.14	15	2.4	0.047
6	5.9	0.12	16	2.2	0.043
7	5.2	0.10	17	2.1	0.041
8	4.4	0.086	18	2.0	0.039
9	4.0	0.078	19	1.9	0.037
10	3.6	0.070	20	1.8	0.035

Current Direction:

- In a westward-flowing current the dynamic height anomaly along an isobaric surface increases toward the Poles in both Hemispheres.

- In an eastward-flowing current the dynamic height anomaly along an isobaric surface decreases toward the Poles in both Hemispheres

Figure 7 shows that the currents in the region are almost entirely zonal. North of 9° N. the presence of the westerly-flowing North Equatorial Current is evident, with maximum velocities of about 0.3 knots in the western section and 0.2 knots in the eastern one. The Current also appears to be narrower to the west, indicating that

it accelerates, grows narrower, and turns somewhat southward between about 155° W. and 165° W. The boundary between the North Equatorial Current and the Countercurrent appears to be quite sharp and is at 9° N. in both meridional sections on Figure 7. The Countercurrent is shown on Figure 7 as an eastward-flowing current between 3°-5° N. and 9° N.; it is broader in the west and somewhat slower-moving than in the eastern section; maximum velocities are about 0.7 knots in the 150°-160° W. section and 0.6 knots in the 160°-170° W. section in Figure 7. South of about 4° N. in both sections there are indications of fairly strong (0.7 knots) westerly-moving currents south to at least 7° S. but within 2 degrees of the Equator in the 150° W.-160° W. section this current is interrupted by easterly flow down to depths of some 400 meters. Almost no indication of this easterly flow is present in the western section. The westerly flow south of 4° N. is, of course, the South Equatorial Current; the eastward-flowing current at the Equator is the Equatorial Undercurrent, or Cromwell Current. The computation of geostrophic currents near the Equator is uncertain, since Coriolis' force vanishes at the Equator and is quite small within 1 or 2 degrees of the Equator; consequently, friction must play an important part in the balance of forces governing the flow, and computed geostrophic current velocities will overestimate the speed of the flow to an uncertain degree. At 1-2° S. between 150° W. and 160° W., Figure 7 shows velocities of about 1.5 to 0.7 knots toward the east. By direct current measurements, Knauss (1960) found velocities of up to 3 knots at the core of the Undercurrent, at 0° latitude, 140° W. longitude. Thus the velocities computed at these latitudes from Figure 7 seem to be approximately correct, but not too much dependence should be put on computed geostrophic current velocities at latitudes of less than about 2°.

It is evident from Figure 7 that the Undercurrent must in part originate somewhere between 150° W. and 170° W. Both the east- and the west-flowing currents show evidence of acceleration downstream in the Line Islands region. It can also be seen that the major equatorial currents are essentially surface currents, with velocities diminishing to small values at depths of 300 meters or more. Before leaving Figure 7, an explanation should be given of the reason for the discrepancy between the computed geostrophic currents and the observed surface drifts shown in Figures 2-6. At the surface, and at depths down to perhaps 100 meters in the equatorial region, the effects of wind stress make themselves felt. The observed currents are resultants of the currents due to wind stress and the currents due to internal pressure gradients. Thus, for example, although easterly flow is shown at the surface on both sides of the Equator near 155° W. in Figure 7, this geostrophic current is opposed by the Southeast Trades near the Equator, with the result that the currents at the surface lack any sign of an eastward component on charts showing average surface flow conditions. However, there are numerous reports of easterly flow at the surface near the Equator during periods of slack Trades, particularly in the eastern portions of the Pacific.

PHYSICAL AND CHEMICAL PROPERTIES

The observed values of temperature, salinity, and dissolved oxygen are summarized in Figures 8, 9, and 10 as vertical north-south sections, and in Figures 11, 12, 13, and 14 as charts showing the depth of a series of sigma-t surfaces (surfaces of potential density) and properties along these surfaces. Surfaces of equal potential density have dynamic significance because they are quasi-isentropic surfaces and mixing can be assumed to occur preferentially along such surfaces. It can also be assumed that currents tend to flow along surfaces of equal potential density.

The values of depth, temperature, salinity and dissolved oxygen used in drawing figures 8-14 were obtained by machine computation. A new method of interpolation was developed during 1961 which made it possible to obtain interpolated values of the depth of selected surfaces of potential density, and of the water properties on each such density surface, using observed oceanographic station data. This method of interpolation minimizes the effects of internal waves on the interpolated values of temperature, salinity, and dissolved oxygen, and retains these effects in the interpolated values of the depths of the density surfaces. The interpolation is a linear one, which means that the machine interpolation can be duplicated graphically by drawing straight lines between observed values of temperature and salinity on a temperature-salinity diagram. Use of a linear interpolation procedure also means that no spurious maxima and minima are introduced into the interpolated values, as often happens in other interpolation techniques using quadratic or higher-order equations. Once the interpolated values for each station have been obtained, the data are grouped by geographic area, and by month or by season if desired, and the values on each density surface are then averaged. For this report, the data were averaged by areas of 2° of latitude and 10° of longitude; e.g., all interpolated station data between the Equator and 2° N., and between 150° W. and 160° W., were treated as a unit and averaged, with the average values plotted as one single "station" located at 1° N., 155° W. The result is a summary representative of all the data collected in the area, in which the effects of short-term disturbances such as internal waves are minimized, as are the effects of other random variables. The values thus obtained are of course no better than the observed data used to obtain the averaged values, but the technique emphasizes persistent features, summarizes large quantities of data in an objective manner, and introduces less "noise" than any other method now available for rapid processing of large amounts of data.

Figure 8 shows the temperature distribution in the Line Islands area in the form of two north-south vertical sections. In the equatorial Pacific, temperature is the major determinant of density, so that the slope of the isotherms is a good indication of the density distribution and thus of the current structure. The downward slope of the isotherms north of 10° N. is associated with

the westward-flowing North Equatorial Current, for example. It should be noted that between 15° C. and 25° C. the interval between isotherms is 5° C.; elsewhere in Figure 8 it is 1° C. Note the presence of cooler water at the surface near the Equator; it is a result of vertical mixing and probably some surface divergence which brings water of higher density, lower oxygen content, and somewhat higher plant nutrient content to the surface at this latitude. This accounts for most of the enrichment in the biota which is observed at the Equator and discussed in a later section.

Figure 9 shows the corresponding salinity distribution in the two north-south sections in the region of interest. Water of very high salinity is found at a depth of about 150 meters in the South Pacific. Despite the vertical mixing which is characteristic of the Equator, some of this high salinity water is present north of the Equator, at latitudes of up to 8° or 10° N. Therefore this salinity maximum is being carried to the west by the South Equatorial Current, and toward the east by the Undercurrent and Countercurrent. The low surface salinity in the Countercurrent probably accounts for the disappearance of this South Pacific salinity maximum near 9° N., through the effects of vertical mixing. It should be noted that the extreme vertical temperature gradients in the Countercurrent imply great stability, and as a consequence vertical mixing must be greatly inhibited, but not entirely absent. Another near-surface salinity maximum can be detected in Figure 9, north of 9° N. latitude. This maximum is the North Pacific counterpart of the South Pacific maximum, and has its origin at the high-salinity surface water found near 25° N. This maximum is present on a surface which has a slightly higher density than that at the core of the South Pacific salinity maximum. The salinity minimum at a depth of about 750 meters to the south is characteristic of the Equatorial Water Mass (Sverdrup et al. 1942). The maximum at about 250 meters between 4° N. (approximately) and 13° N. marks the boundary between the deeper Equatorial Water Mass and the surface water types of the Countercurrent and the North Pacific Central Water. To the north of 14° N., the entire water column shown in Figure 9 is made up of North Pacific Central Water; the salinity minimum which is found at a depth of about 300 meters near 17°-20° N. and at lesser depths to the south down to about 10° N. is characteristic of North Pacific Central Water (Sverdrup et al. 1942).

Figure 10 shows two vertical north-south sections of dissolved oxygen. South of the Equator, between 160° and 170° W., not enough data were available to permit drawing the dissolved oxygen isopleths. The most important feature shown on Figure 10 is the intense oxygen minimum which is centered at depths of about 400 meters to the east, and 250 meters in the western section, at latitudes of 12° N. and 9° N., respectively. This minimum originates farther east, is carried to the west by the North Equatorial Current, and diminishes in intensity as it goes, owing to mixing with waters of higher oxygen content. Three distinct minima can be detected, on three different potential density levels, in the North Pacific and in most of the portion of the South Pacific shown in the figure.

A fourth, minor minimum is present at 250 meters at 9° S. in the section between 150° W. and 160° W.; no minimum is present elsewhere in these sections at the same density level, so this minimum doubtless has its origin in the South Pacific. The apparent effects of countercurrent cycling of water between the east- and west-flowing currents at the Equator can be seen in the distribution of the oxygen minima with latitude. For example, the deepest minimum, at about 650 meters depth in the eastern section, is present north of 11° N., absent from 10° N. to 6° N., and then reappears between 3° N. and 5° N. It is absent between 2° N. and 2° S., and occurs once more south of 3° S. The simplest hypothesis which would account for this distribution is that the water in the density layer of this minimum is carried westward in the North Equatorial Current, with some horizontal mixing at the junction of this current and the Countercurrent, and that this water which enters the Countercurrent is returned to the east, mixes with the Undercurrent and then with the South Equatorial Current, in which it finally is carried westward. In the absence of significant vertical mixing this would be the most acceptable hypothesis. However, knowledge of mixing processes in the ocean is extremely limited, and the alternative hypothesis, that vertical mixing introduces oxygen into this layer and destroys the minimum at some latitudes, cannot be rejected.

Figure 11 shows the depth of the surface having a potential density of 1.02300 kilograms per liter (sigma-t of 23.00 grams per liter), and the temperature, salinity, and dissolved oxygen content on this surface, which lies in the uppermost part of the permanent thermocline. The flow of water on this surface can be inferred (except at and very near the sea surface and the Equator) from the depth of the surface. In the Northern Hemisphere, the depth of the surface should be greatest on the right-hand side of the current (facing downstream); the current velocity should be directly proportional to the slope of the surface at any one latitude, and a given slope is associated with a stronger current as the Equator is approached. These rules are a consequence of the assumption that the flow is geostrophic (see the section on Currents, this report). Thus, in Figure 11, it can be seen that the Countercurrent is present at 6° N. to about 9° N., since the deepest part of the surface is found south of 6° N. and the shallowest near 9° N. The effects of the South Equatorial Current are evident in the slope of the density surface downward from the sea surface at about 2° N. to more than 90 meters at 3° N. in the western portion of the area. The trough in the density surfaces near 4° N. and the ridge in these surfaces at 9° N. are excellent indications of the presence of the Countercurrent, and can be seen in Figures 11, 12, 13, and 14. The temperature distribution in Figure 11 shows two zonal minima, which are associated with similar minima in the salinity distribution on this surface. These are symptomatic of the excess of precipitation over evaporation which is characteristic of this latitude belt throughout the North Pacific.

Figure 11 shows both annual mean conditions on the density surface with sigma-t equal to 23.00, and the conditions in February

and in July and August. The data for these two months are adequate for showing trends in the seasonal distributions of properties, but the details may not be significant owing to the relatively small amounts of data available during these months. In January the trough just north of the Equator is some 10 meters shallower than the average depth, implying somewhat slower speeds in the Countercurrent. Farther north, the density surface is shallower in January than under average conditions, and the sigma-t surface intersects the sea surface considerably farther south, at about 17° N. below Hawaii, as compared to about 19° N. on the average. In July-August, these conditions are reversed: the density surface is deeper almost everywhere, and extends slightly farther to the north and south before intersecting the sea surface. Some seasonal changes in the distributions of temperature, salinity, and dissolved oxygen are also evident; salinities in the northern areas are lower than average in February, and so are the temperatures, while in July-August the opposite holds true. In the July-August chart there is also a most interesting suggestion of influx of high-salinity, high-temperature, and low-oxygen water along this density surface from the southwest. It is, however, possible that this effect is an artifact due to the relatively small amount of data available in the southwest portion of the area during July and August.

Figure 12 shows average conditions on the surface with a potential density of 1.02440 kg./L. (sigma-t 24.40 gm./L.), and conditions in February and in July-August. This layer lies at the core of the South Pacific salinity maximum. The average conditions are analogous to those already discussed in Figure 11: the ridge and trough in the depth of the surface, associated with the Countercurrent; the two low-salinity, low-temperature tongues originating in the east; and some evidence of seasonal changes in these properties on this density surface. It is evident that the seasonal changes are quite small at this level, owing to its location within the thermocline and the resultant vertical stability which in part isolates this layer from changes at the sea surface nearby. One significant exception to this lack of large seasonal changes is the change in dissolved oxygen concentrations near the island of Hawaii. Here it is evident that during the winter there is an influx of water with a high dissolved oxygen content, presumably because this density surface intersects the sea surface somewhat north of 20° N. during winter, and some of the oxygen-saturated high salinity surface water sinks along this density surface when the surface temperatures drop late in the year.

Figure 13 shows conditions on two surfaces, one with a potential density of 1.02540 (sigma-t equal to 25.40), and one with a potential density of 1.02620 (sigma-t 26.20). The latter surface is located in the core of the North Pacific Central water salinity minimum. In these as in the previous such charts, it can be seen that the South Pacific is characterized by water, at a given density surface, of salinity higher than that in the North Pacific. At the levels of the two density surfaces in Figure 13, a strong gradient of

properties can be seen at the Equator, implying gentler mixing at this point; another strong gradient in the distribution of properties on these surfaces is present at the boundary between the Countercurrent and the North Equatorial Current. An analysis of winter-summer differences on the two surfaces in Figure 13 did not reveal any significant differences. Both of these surfaces are deep in the thermocline and well isolated from seasonal changes.

Figure 14 also shows the distribution of properties on two potential density surfaces, with sigma-t values of 26.80 and 27.20. The first surface lies near the center of the shallow North Pacific oxygen minimum, the second at the core of the Equatorial Water Mass salinity minimum and near the deep oxygen minimum. On the shallower surface, sigma-t 26.80, the depth contours still resemble those of the thermocline and shallower surfaces. The interesting features are shown on the oxygen distribution, in which it is evident that the low-oxygen waters originate to the east, and are being carried to the west and slightly south; the intensity of the minimum decreases to the west. A small area in the east at the Equator also shows low oxygen concentrations. To the south and north much higher concentrations of dissolved oxygen are evident. On the surface with sigma-t equal to 27.20, the depth contours no longer show evidence of the presence of the Countercurrent. Instead the topography is rather flat, with little evidence of systematic flow. Temperature and salinity differences become very minor, although there is a dissolved oxygen pattern quite similar to that on the shallower surface in Figure 14.

At greater depths the entire Pacific Ocean is filled with water of such extreme uniformity in salinity that no difference can be detected in this property from New Zealand to Canada, and from Panama to the Philippines. This vast quantity of water originates in the Antarctic, fills four-fifths of the Pacific basin, and is isolated from the surface by the relatively low density of North Pacific surface water and the lack of a pronounced vertical circulation in the North Pacific like that found in the Atlantic, where deep water is formed near Greenland during the winter.

Figure 15 shows surface temperature and salinity values for a number of years from observations taken weekly at Johnston Island, and daily at Christmas Island. The values have been smoothed by Fourier analysis of 15-day mean values. The figure illustrates the seasonal and longer-term changes in both salinity and temperature at these two locations. Annual mean values are shown in the figure by crosses. Christmas Island is characterized by year-to-year changes in salinity and temperature which are as great as, or greater than, the regular seasonal changes. It is interesting to note that the salinity at Christmas Island tends to show two annual minima, particularly in the years 1958 and 1959. The years 1957 and 1958 were years of unusual temperatures over the entire North Pacific, with unusually warm water off the American coast, and cool water near Japan. The Christmas Island temperatures reflect this change, with

a rapid increase in temperature early in 1957, followed by a much more gradual decrease to lower values in subsequent years. At Johnston Island the record is not as long as that at Christmas Island, but a regular seasonal pattern of events can easily be discerned in the temperature data. It is difficult to analyze the salinity curves for Johnston Island; apparently the early part of the year is characterized by rather large fluctuations of salinity, with lesser changes later on. This type of seasonal change is characteristic of Oahu, where a high-salinity area to the north of the island moves southward in winter and causes similar fluctuations by moving into and out of the island vicinity during the winter and early spring. In summer the high-salinity region is farther to the north and the fluctuations become much smaller at the sampling site on Oahu.

PLANKTON

The distribution of the standing crop of zooplankton near the Line Islands has been studied primarily by King and Hida (1954, 1955, 1957) and by King and Demond (1953). There is good evidence of enrichment of the surface waters by nutrients due to upwelling and vertical mixing near the Equator, with subsequent relatively large (by tropical standards) standing crops of zooplankton near the Equator and in the Line Islands group from Christmas Island to Palmyra Island. The evidence for any seasonal changes in the standing crop is weak, and can be summarized by saying that in the northern summer (June through November) maximal abundances of zooplankton are found in the southeast of the region of interest, from about 2° S., 150° W., to the area near Palmyra Island, and also near Hawaii; standing crops of more than 50 cubic centimeters per thousand cubic meters of water strained are common in these areas at that time. In the northern winter (December through May), the areas of maximal abundance remain about the same, but standing crops drop to between 50 and 25 cc./1,000 $m.^3$. In all cases the areas to the south of the Equator and those to the northwest of the Line Islands yielded estimates of standing crops of less than 25 cc./1,000 $m.^3$.

Zooplankton species characteristic of island lagoons can be used as indicators of water exchange between the lagoon and outside waters. The lagoon at Christmas Island contains large numbers of a copepod, Macandrewella, which is the dominant copepod in the lagoon and could be used as an indicator organism. This new species is being described by Jones and Park (in manuscript). A new species of Centropages has been found in the lagoon waters of Palmyra and in the inshore waters of Johnston Island. This endemic form common to these two islands may indicate that the islands are in a common current.

Table 3.--Oceanographic station data used in preparing Figures 7-14

Cruise		Date	Hydrographic stations
Hugh M. Smith	1	December 1949	1-16
	2	January-March 1950	4-21, 35-52
	5	June-August 1950	5-22, 33-50
	8	January-March 1951	2-19, 27-69, 88-105
	10	July 1951	11-12, 23-29
	11	August-October 1951	33-50
	12	October-November 1951	11-12, 23-28
	14	January-March 1952	1-16, 35-47
	16	July-August 1952	1-17, 26-28, 30
	17	September 1952	11-13, 23-28
	19	January 1953	26-50
	20	March 1953	17-18, 31, 42-50, 58-64
	21	August 1953	13, 35-38, 49-60
	26	June 1954	7, 9, 11, 13, 15, 17, 19, 21, 23, 25, 25a, 27, 29, 29a, 31
	34	April-June 1956	2-9, 117-125
	35	August-September 1956	1-12, 70-79, 122, 123, 125-128
	38	January-March 1957	54-57
Albatross (Swedish Deep-Sea Expedition)		November-December 1947	105, 108, 111-112, 123, 126-130
Dana		October 1928	3585
Carnegie	VII	November 1929	157-159

BIBLIOGRAPHY

I - Geophysical

ARTHUR, R. S.
1960. A review of the calculation of ocean currents at the Equator. Deep-Sea Research, vol. VI, no. 4, p. 287-297.

AUSTIN, T. S.
1954. Mid-Pacific oceanography, Part V. Transequatorial waters, May-June 1952, August 1952. U.S. Fish and Wildl. Serv., Spec. Sci. Rept. - Fish., 136: 85 p.

AUSTIN, T. S., E. D. STROUP, and M. O. RINKEL
1956. Variations in the Equatorial Countercurrent in the central Pacific. American Geophysical Union, Transactions 37(5): 558-564.

AUSTIN, T. S.
1957. Summary, oceanographic and fishery data, Marquesas Islands area, August-September 1956 (EQUAPAC). U.S. Fish and Wildl. Serv., Spec. Sci. Rept. - Fish. 217: 186 p.

AUSTIN, T. S. and M. O. RINKEL
1957. Variations in upwelling in the Equatorial Pacific (Abstract), Ninth Pacific Science Congress. Abstract of papers, p. 168.

AUSTIN, T. S.
1958. Variations with depth of oceanographic properties along the Equator in the Pacific. Transactions, American Geophysical Union 39(6): 1055-1063.

AUSTIN, T. S.
1959. Secular warming in sea surface temperatures, equatorial Pacific, 1955-1958. Proceedings, Hawaiian Academy of Science, 34th Annual Meeting, Abstract p. 21.

AUSTIN, T. S. and V. E. BROCK
1959. Meridional variations in some oceanographic and marine biological factors in the central Pacific. American Association for the Advancement of Science. Abstract p. 130-131.

AUSTIN, T. S.
1960. Oceanography of the east-central equatorial Pacific as observed during Expedition EASTROPIC. U.S. Fish and Wildl. Serv., Fishery Bulletin 168: 257-282.

AUSTIN, T. S.
1960. Summary - 1955-57 ocean temperatures, central equatorial Pacific. California Co-operative Oceanic Fisheries Investigations Reports. 1 January 1958 to 30 June 1959, 7: 52-55.

BARKLEY, R. A. and T. S. AUSTIN
1961. Distribution of properties about the Equatorial Undercurrent. (Abstract) Tenth Pacific Science Congress. Abstract of Symposium Papers, p. 339-340.

BRUNEAU, L., N. G. JERLOV, and F. F. KOCZY
1953. Physical and chemical methods. Reports of the Swedish Deep-Sea Expedition, vol. III, no. 4, p. 99-112. Göteborg.

BURKOV, V. A.
1961. Investigation of currents in the western tropical part of the Pacific during the International Geophysical Year, 1957-1958. (Abstract) Tenth Pacific Science Congress. Abstract of Symposium Papers, p. 340.

CHARNEY, J. G.
1960. Non-linear theory of a wind-driven homogeneous layer near the Equator. Deep-Sea Research, vol. VI, no. 4, p. 303-310.

COCHRANE, J. D.
1956. The frequency distribution of surface-water characteristics in the Pacific Ocean. Deep-Sea Research, vol. IV, p. 45-53.

COCHRANE, J. D.
1958. The frequency distribution of water characteristics in the Pacific Ocean. Deep-Sea Research, vol. V, p. 111-127.

CROMWELL, T.
1951. Mid-Pacific oceanography, January-March 1950. U.S. Fish and Wildl. Serv., Spec. Sci. Rept. - Fish. 54, 9 p.

CROMWELL, T.
1953. Circulation in a meridional plane in the central equatorial Pacific. Journal of Marine Research 12(2): 196-213.

CROMWELL, T. and T. S. AUSTIN
1954. Mid-Pacific oceanography II, by T. Cromwell, and mid-Pacific oceanography III, by T. S. Austin. U.S. Fish and Wildl. Serv., Spec. Sci. Rept. - Fish. 131 (Part II: 13 p., Part III, 17 p.)

CROMWELL, T., R. B. MONTGOMERY, and E. D. STROUP
1954. Equatorial undercurrent in Pacific Ocean revealed by new methods. Science 119(3097): 648-649.

CROMWELL, T. and J. L. REID, JR.
1956. A study of oceanic fronts. Tellus 8(1): 94-101.

DEFANT, A.
1961. Physical oceanography. Vol. 1. New York, Pergamon Press, 729 p.

FLEMING, J. A., C. C. ENNIS, H. U. SVERDRUP, S. L. SEATON, and W. C. HENDRIX
1945. Scientific results of cruise VII of the Carnegie during 1928-1929 under the command of Captain J. P. Ault. Oceanography I-B, observations and results in physical oceanography. Carnegie Institution of Washington publication 545, 315 p.

FOFONOFF, N. P. and R. B. MONTGOMERY
1955. The Equatorial Undercurrent in the light of the vorticity equation. Tellus 7; 518-521.

HIDAKA, K. and Y. NAGATA
1958. Dynamical computation of the equatorial current system of the Pacific, with special application to the Equatorial Undercurrent. Geophys. J. 1, p. 198-207.

JERLOV, N. G.
1951. Optical studies of sea-water. Reports of the Swedish Deep-Sea Expedition, vol. III, no. 1, p. 1-57. Göteborg

JERLOV, N. G.
1953. Particle distribution in the ocean. Reports of the Swedish Deep-Sea Expedition, vol. III, no. 3, p. 73-97. Göteborg.

JERLOV, N. G.
1953. Studies of the equatorial currents in the Pacific. Tellus 5(3): 308-314.

JERLOV, N. G.
1956. The equatorial currents in the Pacific Ocean. Reports of the Swedish Deep-Sea Expedition, vol. III, no. 6, p. 129-154.

JERLOV, N. G.
1959. Maxima in the vertical distribution of particles in the sea. Deep-Sea Research, vol. V, no. 3, p. 173-184.

KING, J. E., T. S. AUSTIN, and M. S. DOTY
1957. Preliminary report on Expedition EASTROPIC. U.S. Fish and Wildl. Serv., Spec. Sci. Rept. - Fish. 201: 155 p.

KNAUSS, J. A.
1957. An observation of an oceanic front. Tellus 9(2): 234-237.

KNAUSS, J. A. and J. E. KING
1958. Observations of the Pacific Equatorial Undercurrent. Nature 182: 601-602, August 30, 1958.

KNAUSS, J. A.
1960. Measurements of the Cromwell Current. Deep-Sea Research, vol. VI, no. 4, p. 265-286.

KNAUSS, J. A.
1961. Comparison of the equatorial circulation in Atlantic, Pacific, and Indian Oceans (Abstract), Tenth Pacific Science Congress. Abstract of Symposium Papers, p. 341.

KRISS, A. E., S. S. ABYZOV, and I. N. MITZKEVITCH
1960. Micro-organisms as indicators of hydrological phenomena in seas and oceans III. Distribution of water masses in the central part of the Pacific Ocean (according to microbiological data). Deep-Sea Research, vol. VI, no. 4, p. 335-345.

LEIPPER, D. F. and E. R. ANDERSON
1950. Sea temperatures, Hawaiian Island area. Pacific Science 4(3): 228-248.

McGARY, J. W.
1955. Mid-Pacific oceanography. Part VI. Hawaiian offshore waters, December 1949-November 1951. U.S. Fish and Wildl. Serv., Spec. Sci. Rept. - Fish. 152: 138 p.

MONTGOMERY, R. B. and E. PALMÉN
1940. Contribution to the question of the Equatorial Countercurrent. Journal of Marine Research, vol. III, no. 2, p. 112-133.

MONTGOMERY, R. B.
1954. Analysis of a Hugh M. Smith oceanographic section from Honolulu southward across the Equator. Journal of Marine Research, vol. XIII, no. 1, p. 67-75.

MONTGOMERY, R. B.
1961. The Equatorial Undercurrent from geostrophic calculation (Abstract), Tenth Pacific Science Congress. Abstract of Symposium Papers, p. 342.

MURPHY, G. I., K. D. WALDRON, and G. R. SECKEL
1960. The oceanographic situation in the vicinity of the Hawaiian Islands during 1957 with comparisons with other years. California Co-operative Oceanic Fisheries Investigations Reports. 1 January 1958 to 30 June 1959, 7: 56-59.

MUROMTSEV, A. M.
1958. Osnovnye cherty gidrologii Tikhogo Okeana (Principal features of the hydrology of the Pacific Ocean) 632 p. Appendix II (bound separately). Atlas of vertical sections and maps of temperature, salinity, and oxygen content. 124 p. Leningrad. (In Russian.)

REID, J. L. JR.
1961. On the temperature, salinity, and density differences between the Atlantic and Pacific Oceans in the upper kilometre. Deep-Sea Research, vol. VII, no. 4, p. 265-275.

REID, R.O.
1948. The equatorial currents of the eastern Pacific as maintained by the stress of the wind. Journal of Marine Research 7, 74-99.

RICHARDS, A. F.
1958. Trans-Pacific distribution of floating pumice from Isla San Benedicto, Mexico. Deep-Sea Research, vol. V, no. 1, p. 29.

RIEHL, H.
1954. Tropical meteorology. McGraw-Hill Book Company, New York, 392 p.

ROBINSON, A. R.
1960. The general thermal circulation in equatorial regions. Deep-Sea Research, vol. VI, no. 4, p. 311-317.

SCHOTT, G.
1935. Geographie des Indischen und Stillen Ozeans. Hamburg, C. Boysen, 413 p.

SECKEL, G. R.
1955. Mid-Pacific oceanography, Part VII, Hawaiian offshore waters, September 1952-August 1953. U.S. Fish and Wildl. Serv., Spec. Sci. Rept. - Fish. 164: 250 p.

SECKEL, G. R.
1960. Advection - a climatic character in the mid-Pacific. California Co-operative Oceanic Fisheries Investigations Reports. 1 January 1958 to 30 June 1959, 7: 60-63.

SECKEL, G. R.
1961. An atlas of the oceanographic climate of the Hawaiian Islands region. U.S. Fish and Wildl. Serv., Fishery Bulletin 193. (In Press.)

SETTE, O. E.
1955. Consideration of midocean fish production as related to oceanic circulatory systems. Journal of Marine Research, vol. XIV, no. 4, p. 398-414.

SETTE, O. E.
1958. Nourishment of central Pacific stocks of tuna by the equatorial circulation system. Proceedings of the Eighth Pacific Science Congress, 1953, vol. 3: 131-137.

STOMMEL, H.
1957. A survey of ocean current theory. Deep-Sea Research vol. IV, no. 3, p. 149-184.

STOMMEL, H.
1960. Wind drift near the Equator. Deep-Sea Research vol. VI, no. 4, p. 298-302.

STROUP, E. D.
1954. Mid-Pacific oceanography, Part IV, transequatorial waters, January-March 1952. U.S. Fish and Wildl. Serv., Spec. Sci. Rept. - Fish. 135: 52 p.

SVERDRUP, H. U., M. W. JOHNSON, and R. H. FLEMING
1942. The oceans; their physics, chemistry and general biology. New York, Prentice-Hall, 1087 p.

SVERDRUP, H. U.
1944. Results within physical oceanography - scientific results of cruise VII of the Carnegie during 1928-1929 under the command of Captain J. P. Ault. Oceanography I-A, observations and results in physical oceanography. Carnegie Institution of Washington publication 545, 156 p.

THOMSEN, H.
1937. Hydrographical observations. Dana Report No. 12, Copenhagen.

TSUCHIYA, M.
1955a. A simple method for estimating the current velocity at the Equator. Journal of the Oceanographical Society of Japan 11, 1-4.

TSUCHIYA, M.
1955b. A simple method for estimating the current velocity at the Equator. (11) Records of Oceanographic Works in Japan 2, 1-6.

U.S. NAVY HYDROGRAPHIC OFFICE
1947. Atlas of surface currents. Northeastern Pacific Ocean. First edition, H.O. Pub. 570.

U.S. NAVY HYDROGRAPHIC OFFICE
1950. Atlas of surface currents. Northwestern Pacific Ocean. First edition, reprinted (formerly H.O. Misc. 10,058A) H.O. Pub. 569.

U.S. NAVY HYDROGRAPHIC OFFICE
1952. Sailing directions for the Pacific Islands, vol. III, eastern groups, sixth edition, H.O. Pub. 82.

U.S.S.R. MINISTRY OF THE NAVY
1953. Morskoi atlas (marine atlas), vol. II. Physical Geography. Moscow. 76 maps.

VERONIS, G.
1960. An approximate theoretical analysis of the Equatorial Undercurrent. Deep-Sea Research, vol. VI, no. 4, p. 287-296.

WEENINK, M. P. H. and P. GROEN
1952. On the computation of ocean surface current velocities in the equatorial regions from wind data. Konikl. Nederl. Akademie von Wetenschappen, Proceedings (B) 55: 239-246.

WENTWORTH, C. K.
1931. Geology of the Pacific Equatorial Islands. Bernice P. Bishop Museum, B., Occasional Papers, vol. IX, no. 15, p. 1-25, Whippoorwill Expedition Pub. 3, Honolulu, Hawaii.

YOSHIDA, K. HAN-LEE MAO and P. L. HORRER
1953. Circulation in the upper mixed layer of the equatorial North Pacific. Journal of Marine Research, vol. XII, no. 1, p. 99-119.

YOSHIDA, K.
1955. A note on dynamics near the Equator, in view of the recent observations in the eastern equatorial Pacific. Journal of the Oceanographical Society of Japan 11, 1-5.

II - Plankton

BIERI, R.
1959. Distribution of planktonic chaetognatha in the water masses of the Pacific. Limnology and Oceanography, 4(1): 1-28.

GRAHAM, H. W.
1941. Plankton production in relation to character of water in the open Pacific. Journal of Marine Research, vol. IV, no. 3, p. 189-197.

HIDA, T. S. and J. E. KING
1955. Vertical distribution of zooplankton in central equatorial Pacific, July-August, 1952. U.S. Fish and Wildl. Serv., Spec. Sci. Rept. - Fish. 144: 22 p.

INTERNATIONAL GEOPHYSICAL YEAR 1957-1958-1959
1961. Data of oceanological investigations. Research vessel Vityaz, Pacific Ocean, October 1953-March 1959. Vol. V. Plankton. Moscow. (In Russian.)

JONES, E. C.
(MS). The distribution of the genus Candacia (Copepoda: Calanoida) along longitude 160° W., central Pacific.

JONES, E. C. and T. S. PARK
(MS). A new species of Macandrewella (Copepoda: Calanoida) from the lagoon of Christmas Island, central Pacific.

KING, J. E. and J. DEMOND
1953. Zooplankton abundance in the central Pacific. U.S. Fish and Wildl. Serv., Fishery Bulletin 82: 111-144.

KING, J. E.
1954. Variation in zooplankton abundance in the central equatorial Pacific, 1950-1952. Fifth Meeting, Indo-Pacific Fisheries Council, Symposium on Marine and Fresh-water Plankton in the Indo-Pacific, p. 10-17.

KING, J. E. and T. S. HIDA
1954. Variations in zooplankton abundance in Hawaiian waters, 1950-52. U.S. Fish and Wildl. Serv., Spec. Sci. Rept. - Fish. 118: 66 p.

KING, J. E. and T. S. HIDA
1957. Zooplankton abundance in Hawaiian waters, 1953-54. U.S. Fish and Wildl. Serv., Spec. Sci. Rept. - Fish. 221: 23 p.

KING, J. E., T. S. AUSTIN, and M. S. DOTY
1957. Preliminary report on Expedition Eastropic. U.S. Fish and Wildl. Serv., Spec. Sci. Rept. - Fish. 201: 155 p.

KING, J. E. and T. S. HIDA
1957. Zooplankton abundance in the central Pacific, Part II. U.S. Fish and Wildl. Serv., Fishery Bulletin 118: 365-395.

SHERMAN, K.
(MS). Pontellid copepods as possible indicators of surface water types in the North Central Pacific.

WILSON, R. C., E. L. NAKAMURA, and H. O. YOSHIDA
1958. Marquesas area fishery and environmental data, October 1957-June 1958. U.S. Fish and Wildl. Serv., Spec. Sci. Rept. - Fish. 283, 155 p.

YOUNT, J. L.
1958. Distribution and ecologic aspects of central Pacific Salpidae (Tunicata). Pacific Science, 12(2): 111-130.

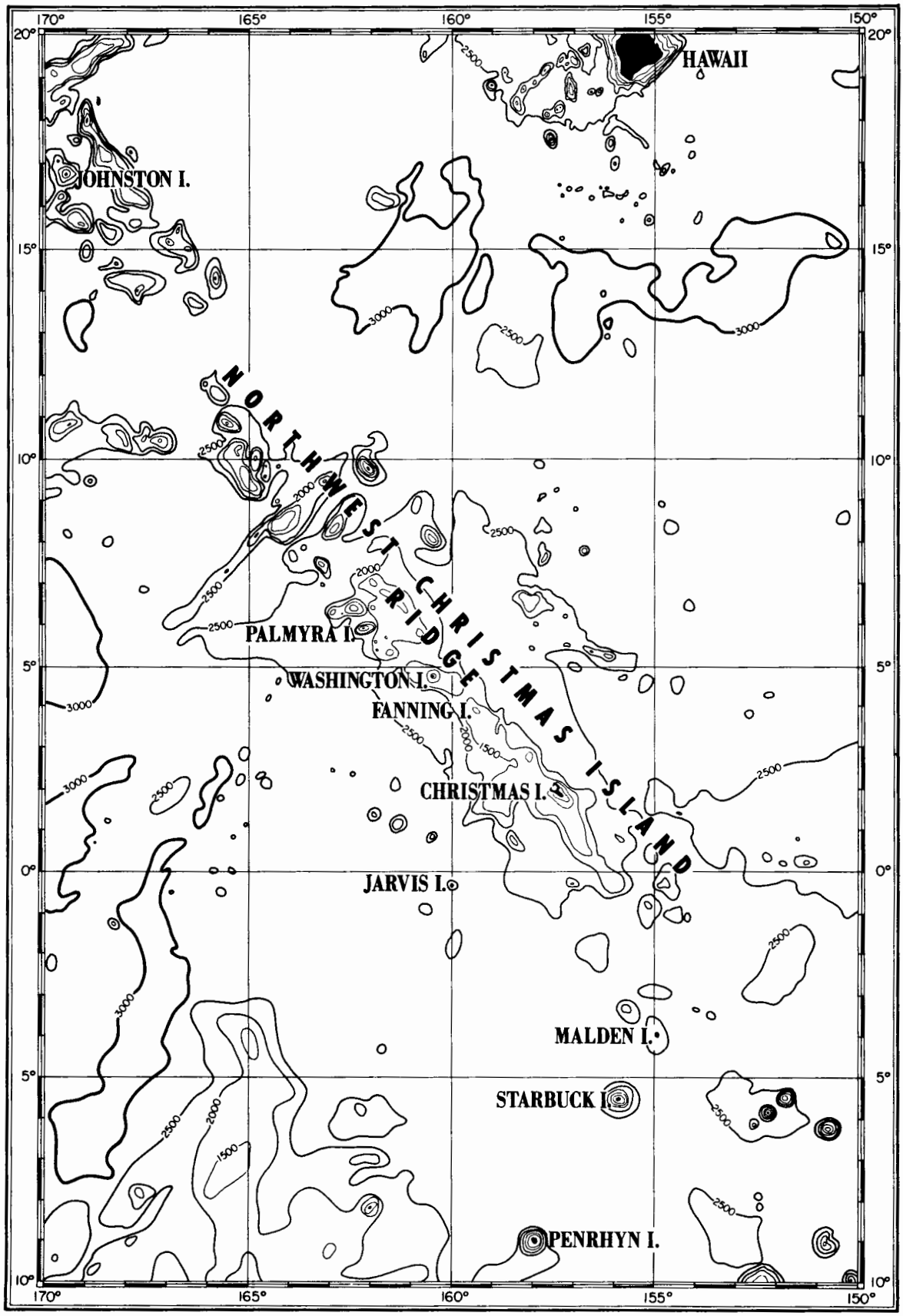

Figure 1.--Bathymetry of the Christmas Island - Johnston Island Area.

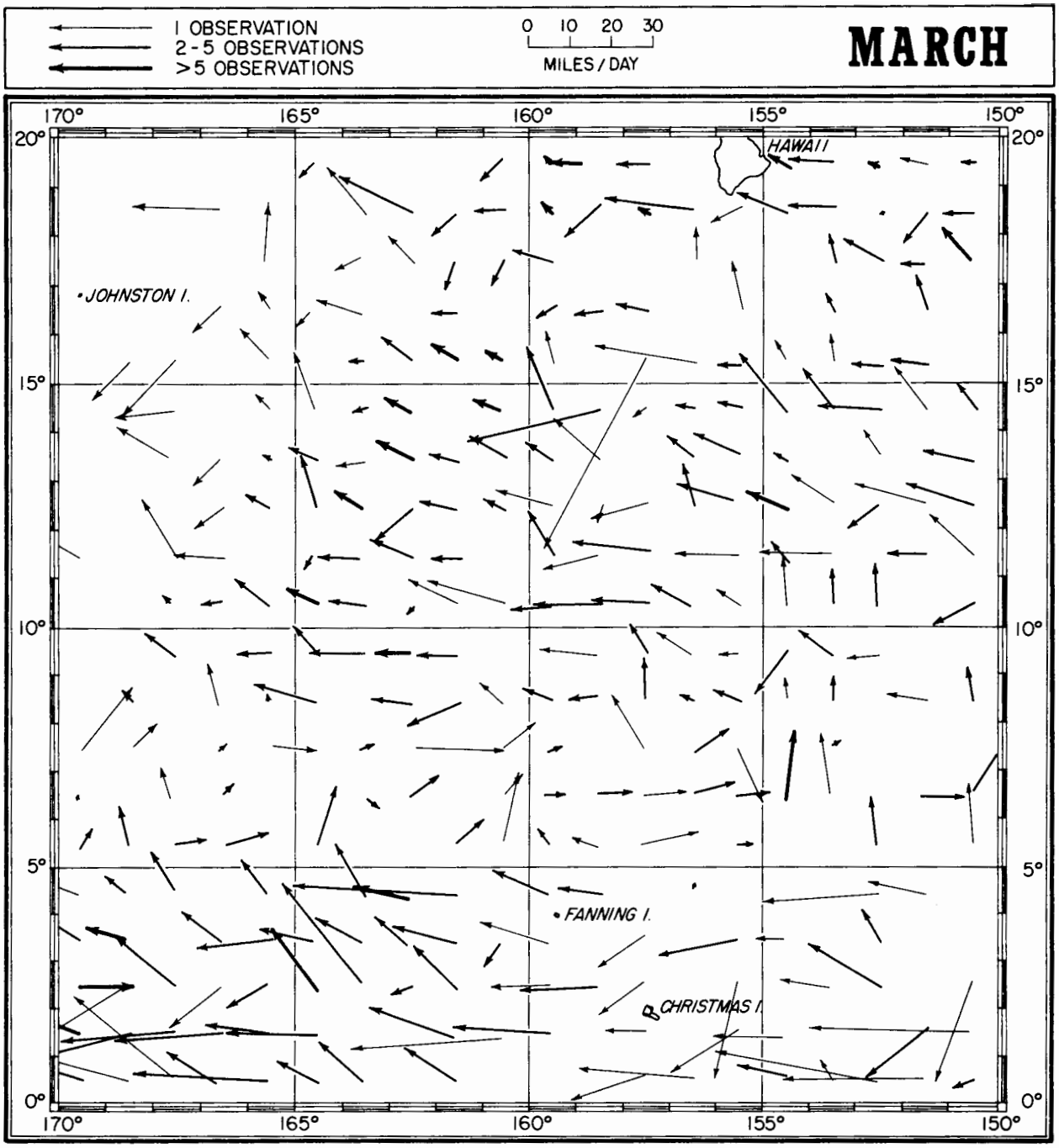

Figure 2.--Surface drift vectors for March.

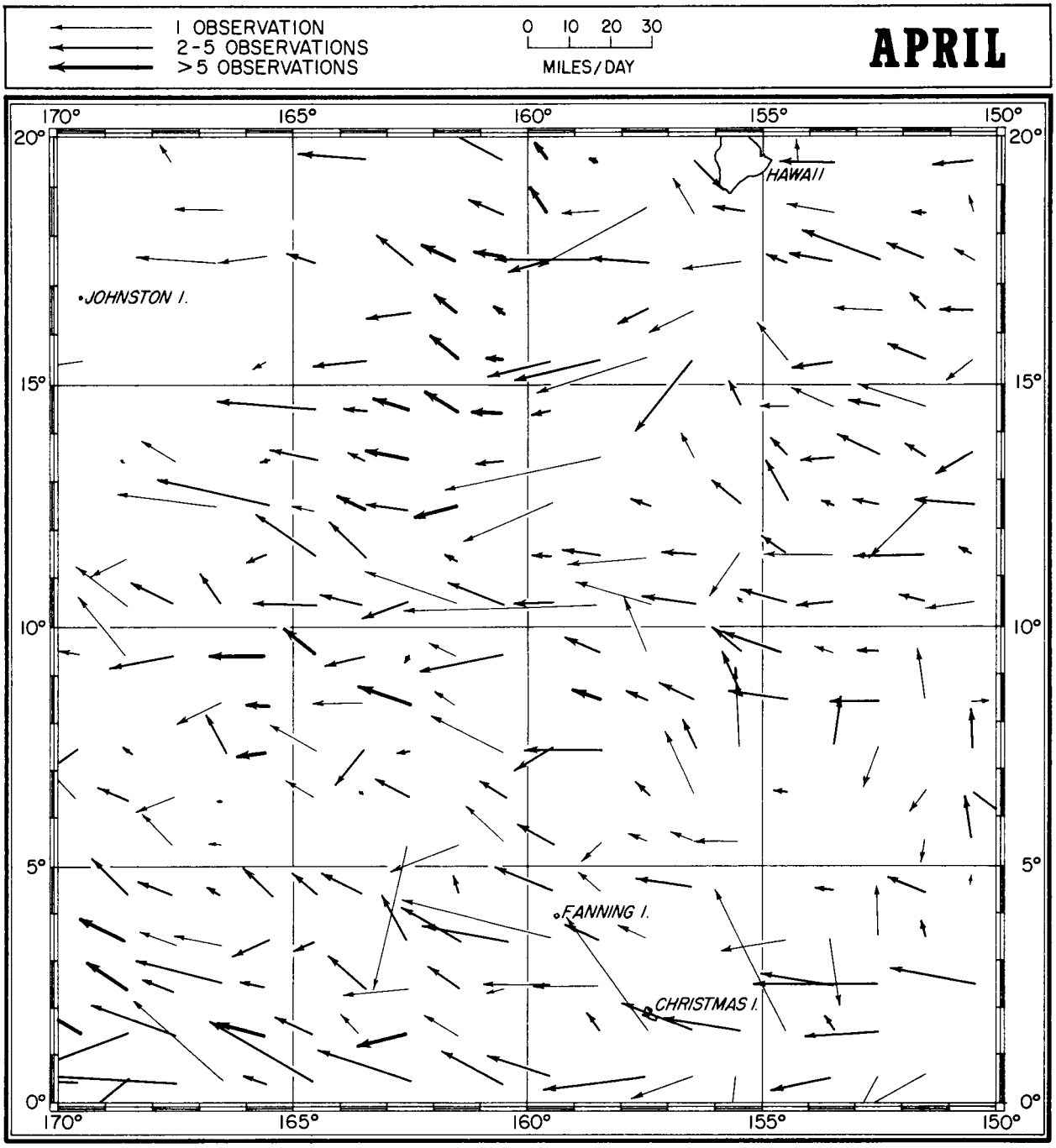

Figure 3.--Surface drift vectors for April.

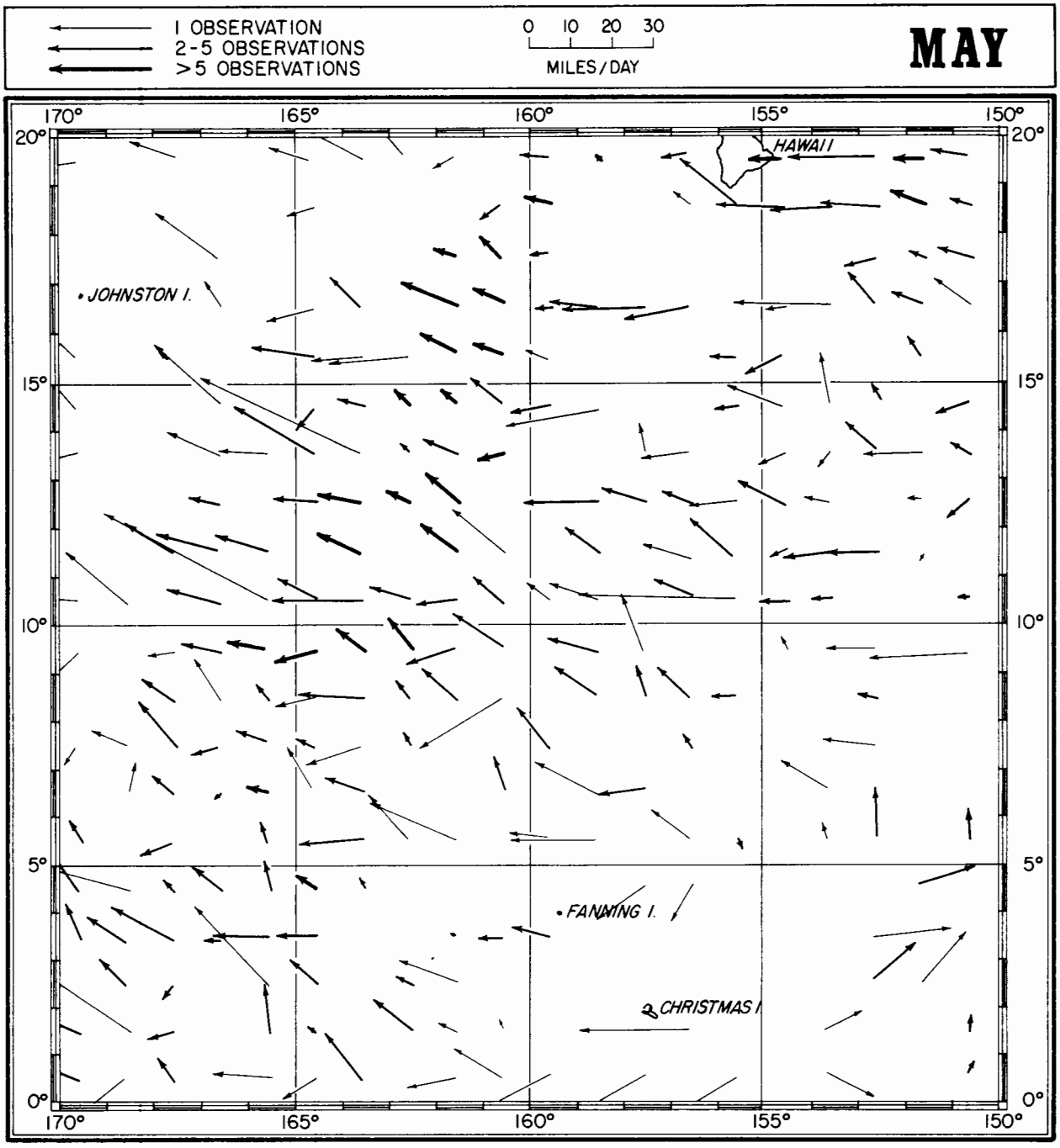

Figure 4.--Surface drift vectors for May.

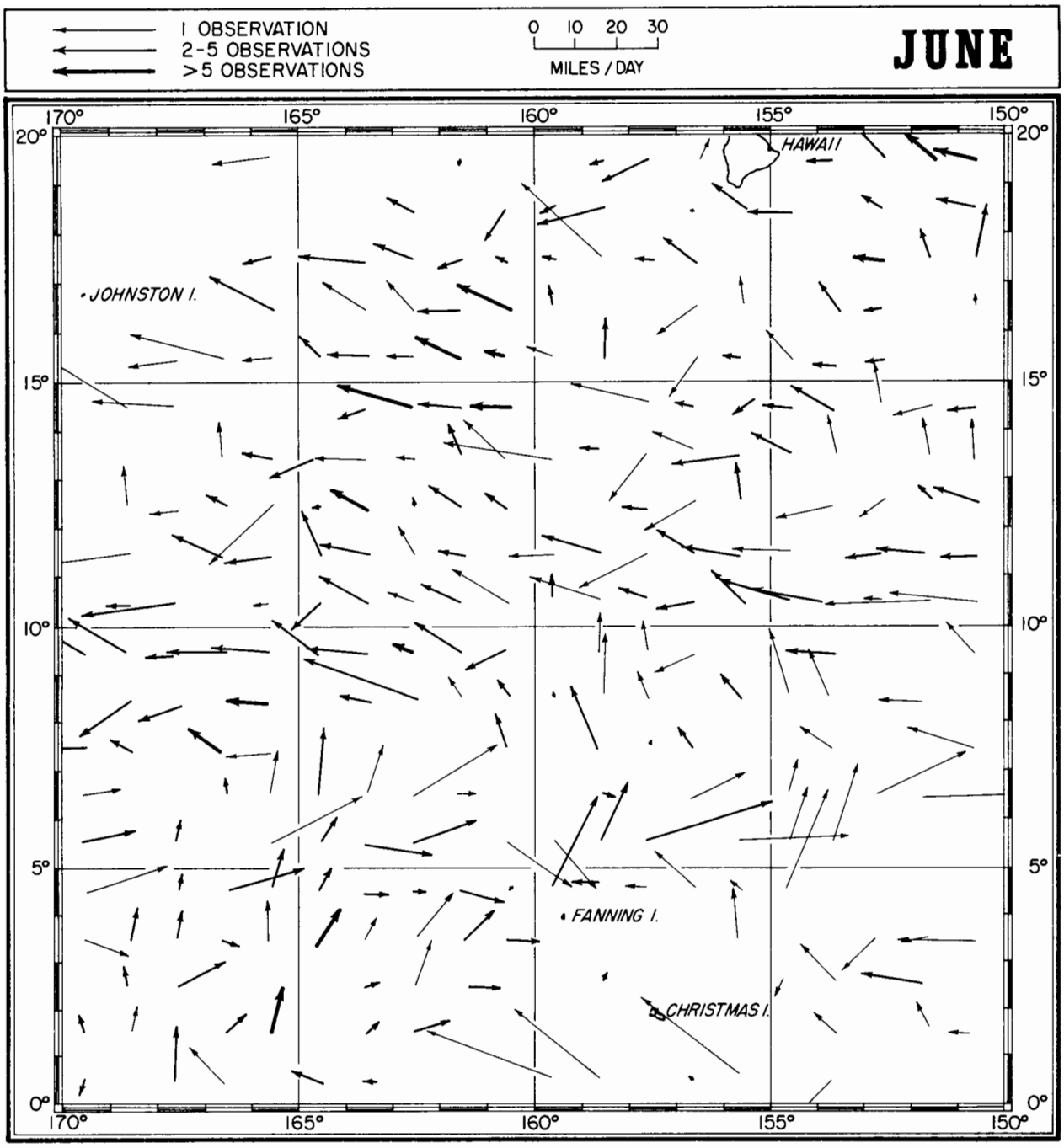

Figure 5.--Surface current vectors for June.

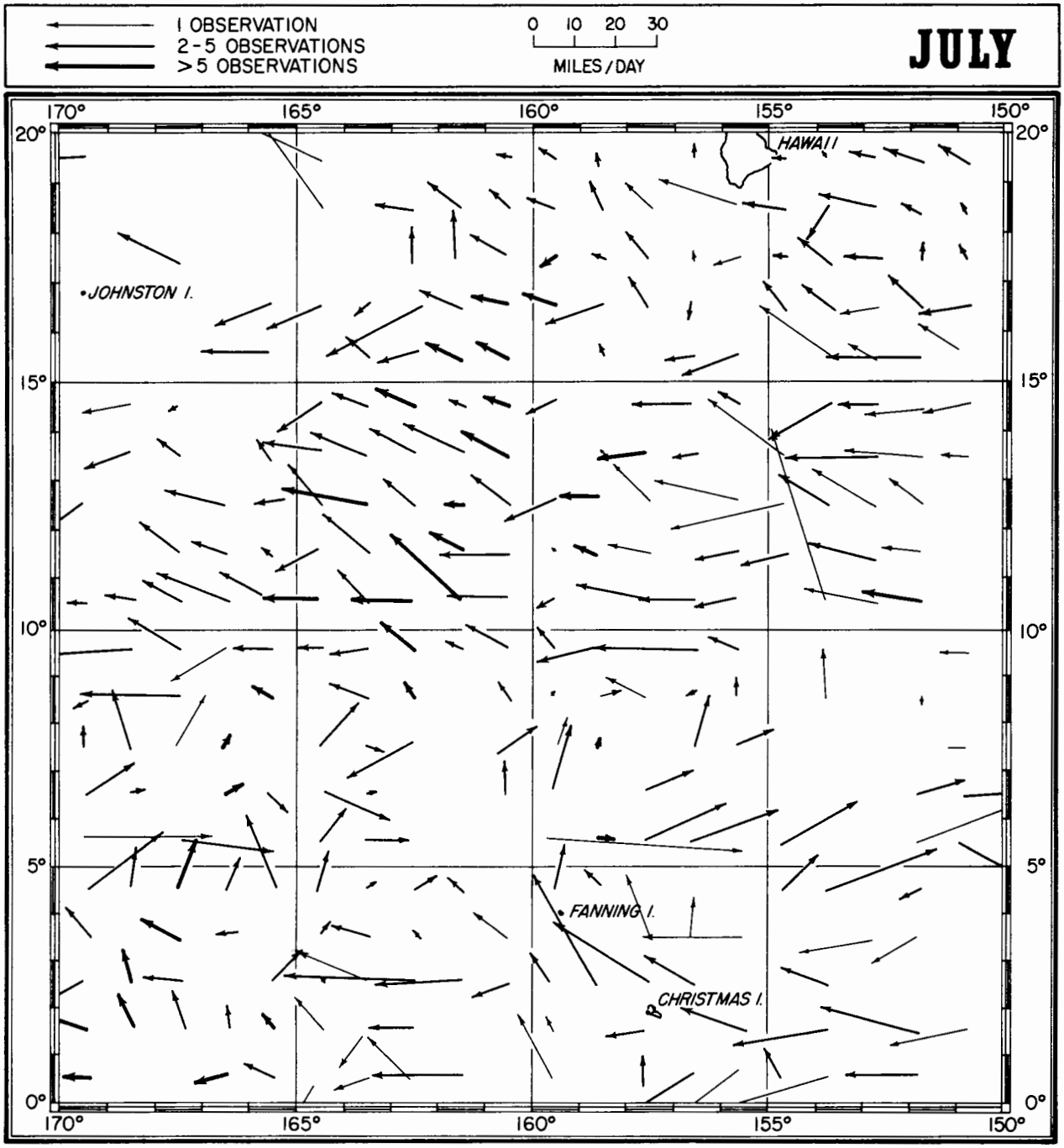

Figure 6.--Surface current vectors for July.

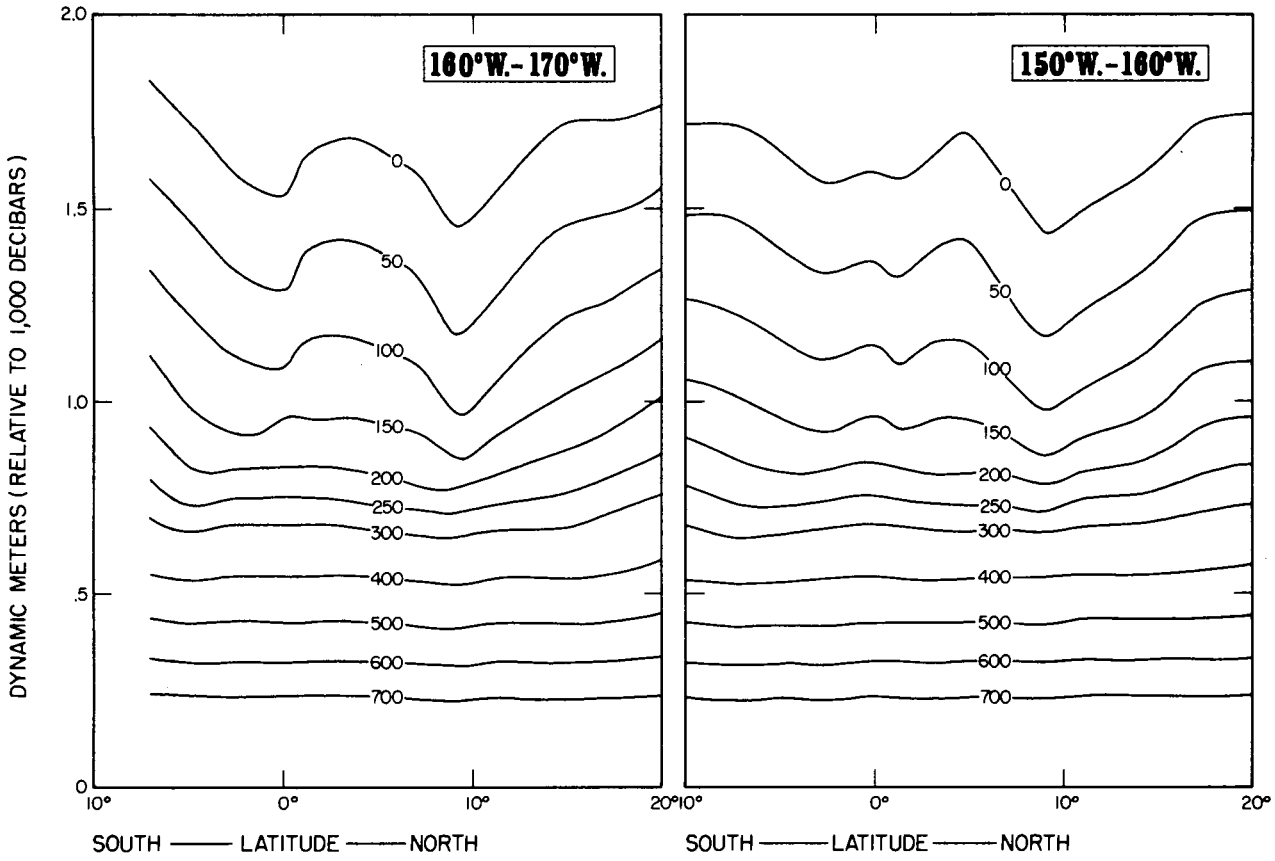

Figure 7.--Dynamic height anomalies relative to 1,000 decibars, based on averages of temperature and salinity in areas of 2° of latitude by 10° of longitude.

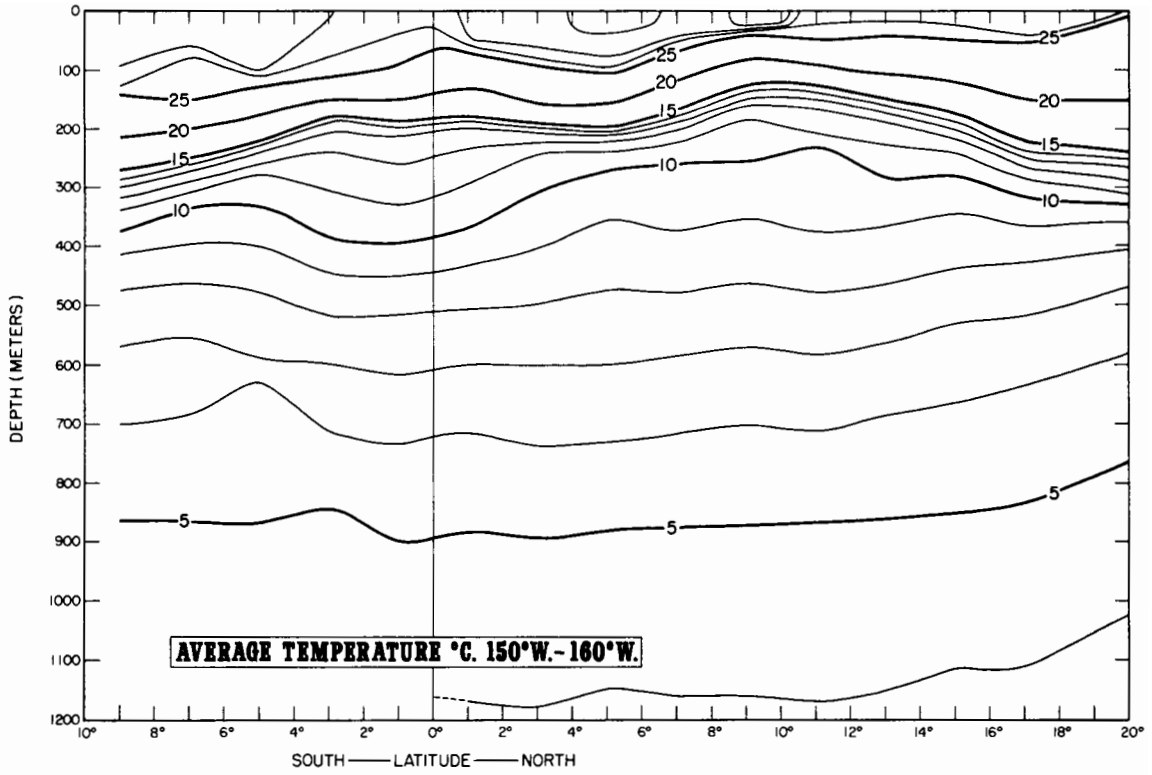

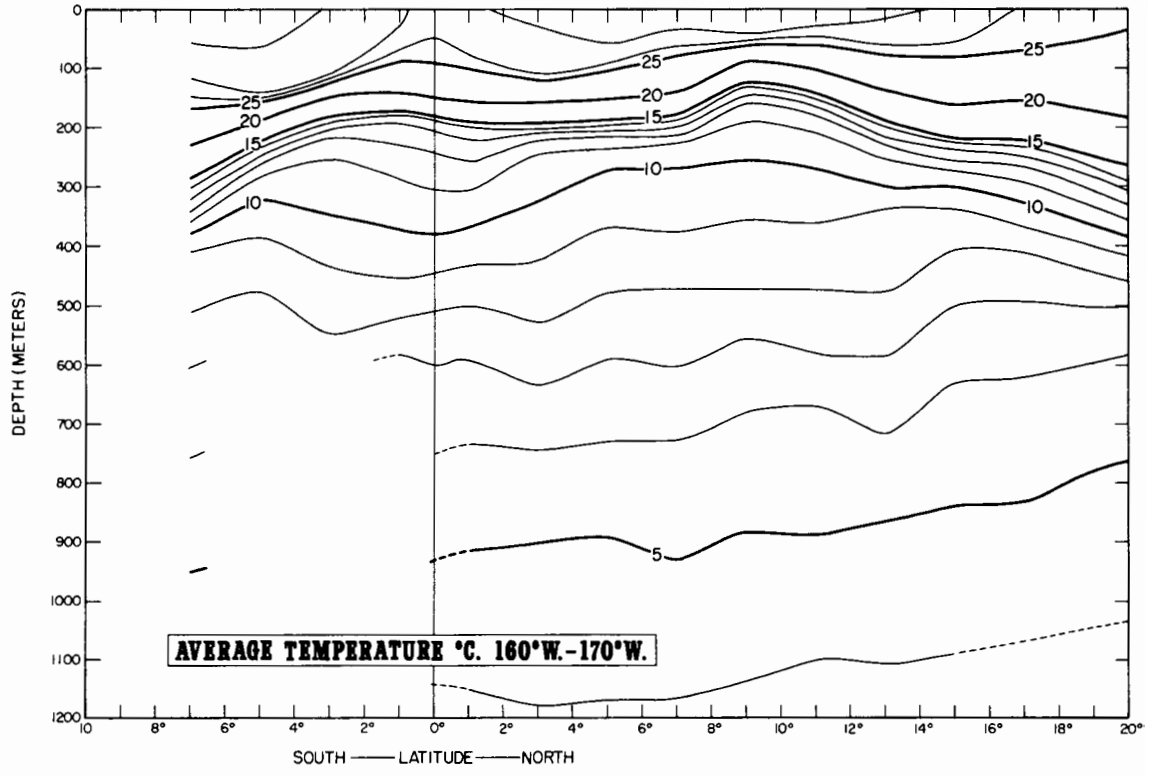

Figure 8.--Meridional temperature sections, based on average values in areas of 2° of latitude by 10° of longitude.

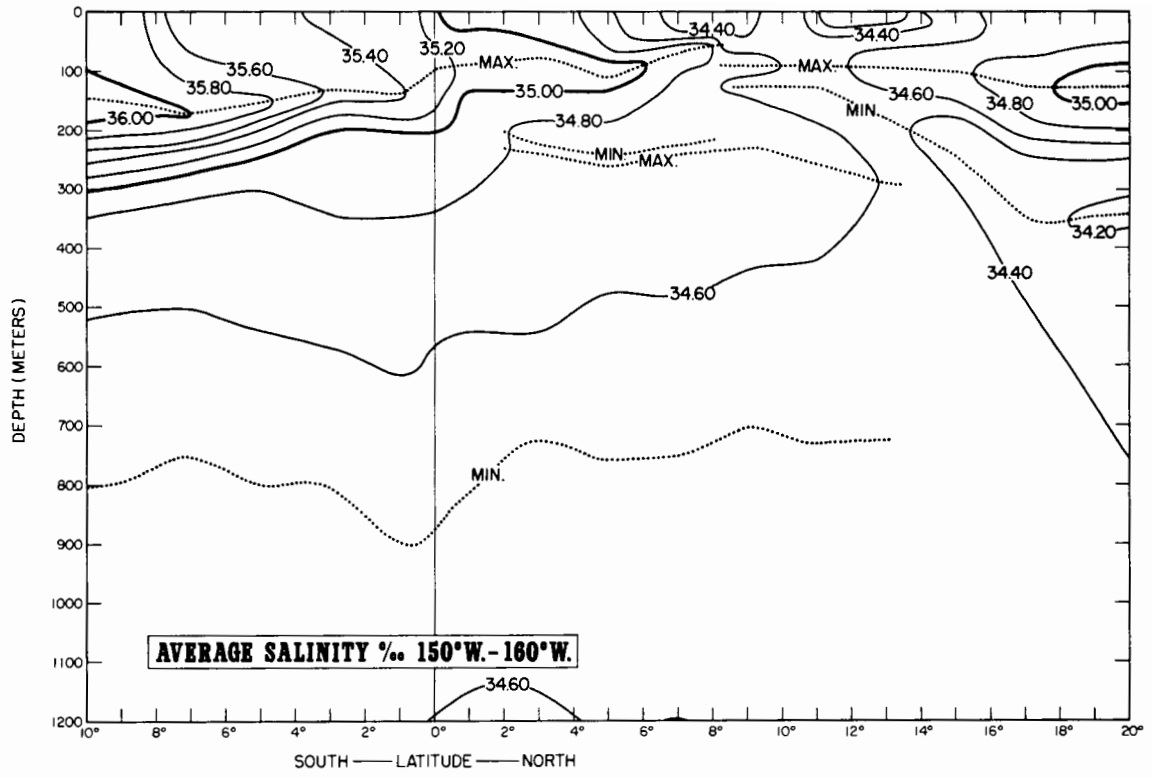

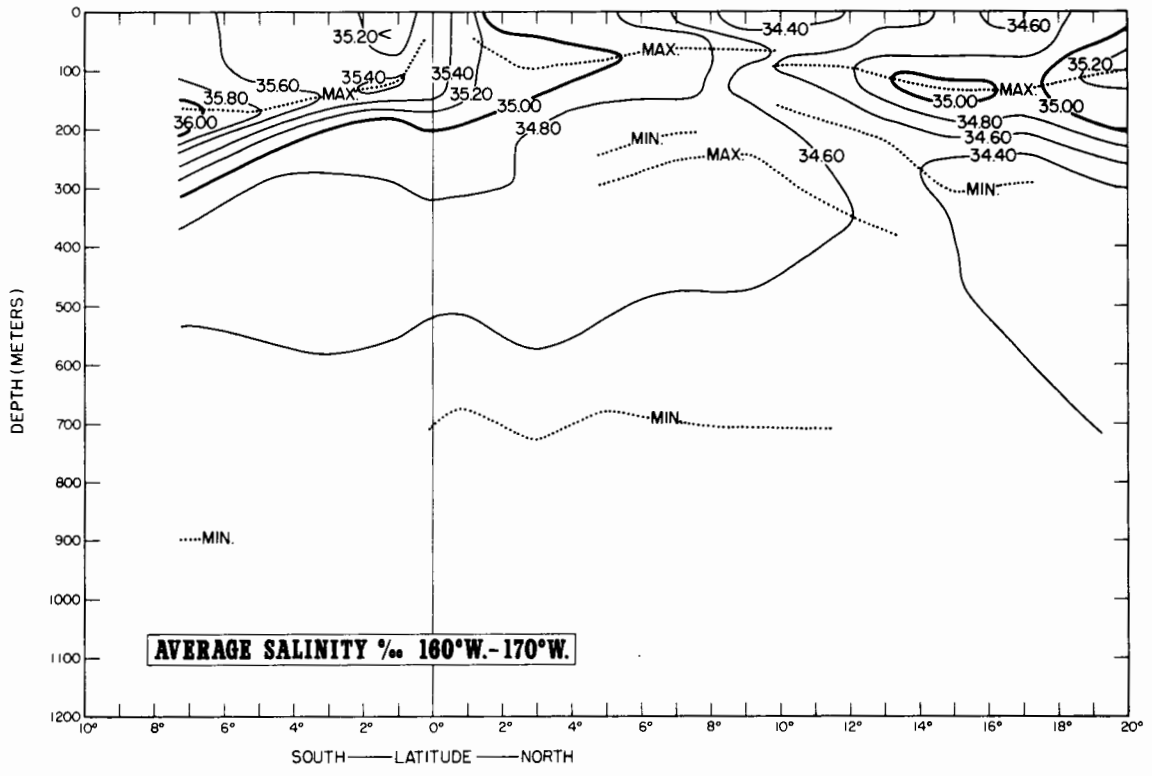

Figure 9.--Meridional salinity sections, based on average values in areas of 2° of latitude by 10° of longitude.

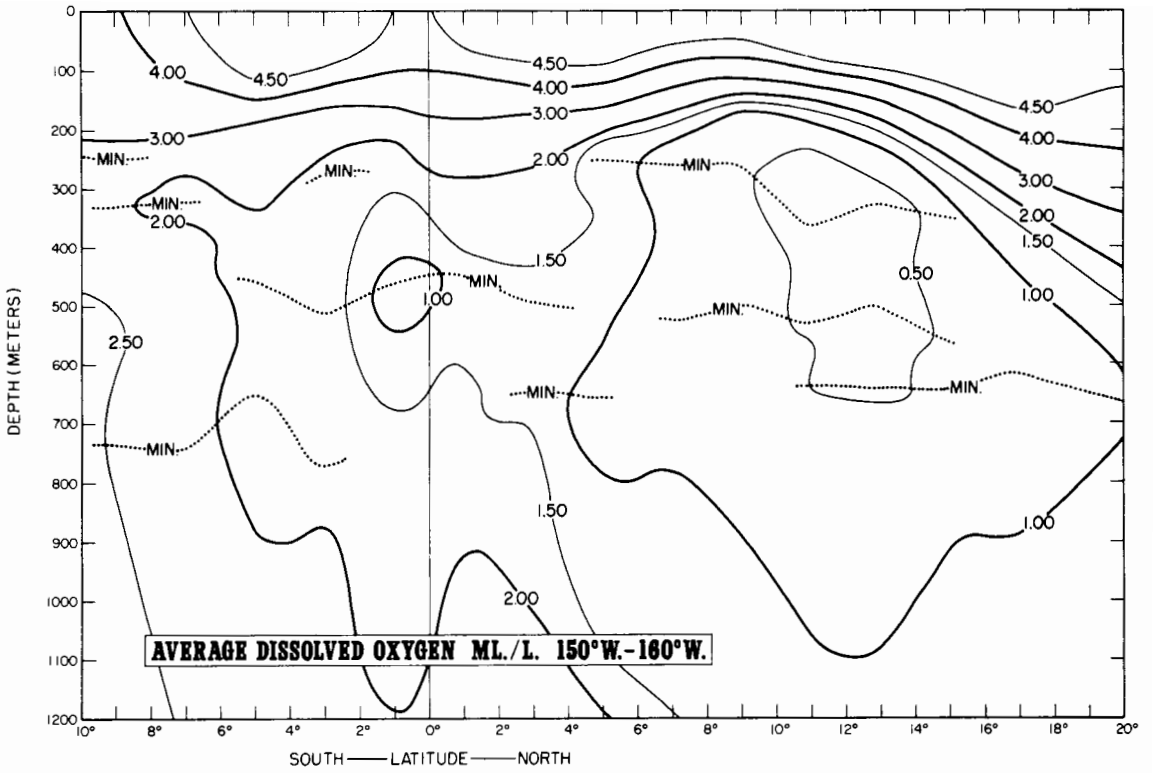

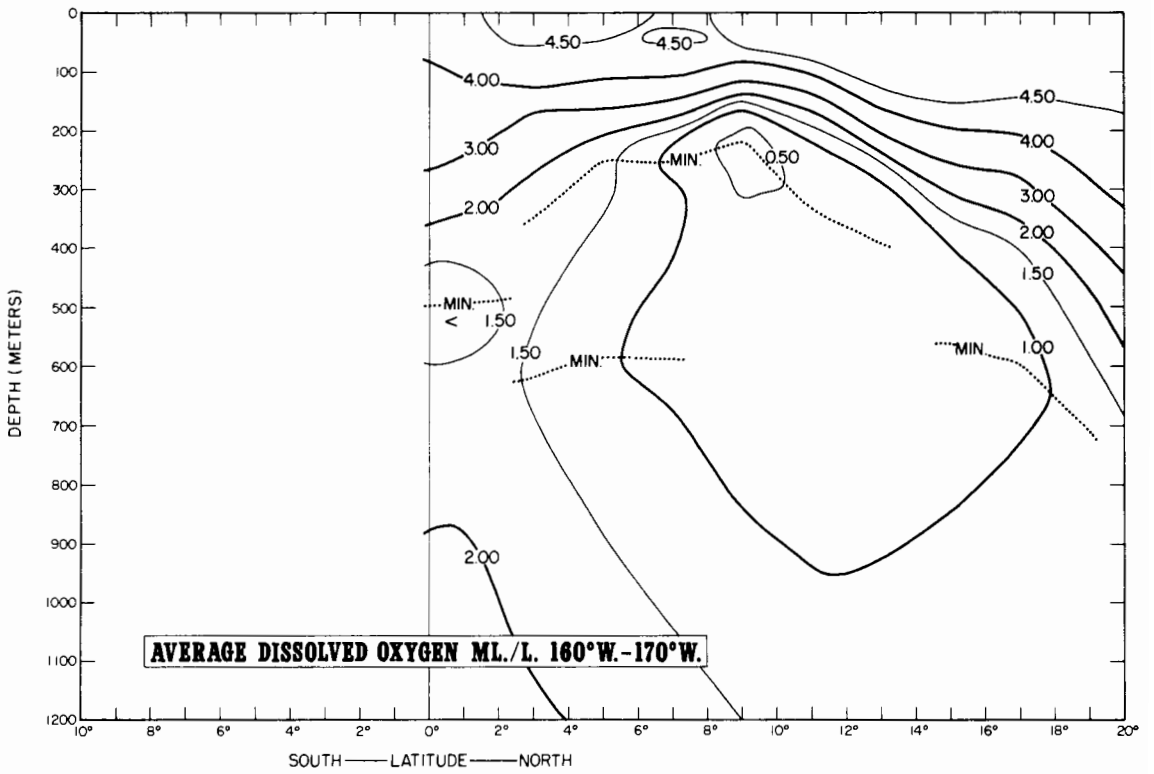

Figure 10.--Meridional dissolved oxygen sections, based on average values in areas of 2° of latitude by 10° of longitude.

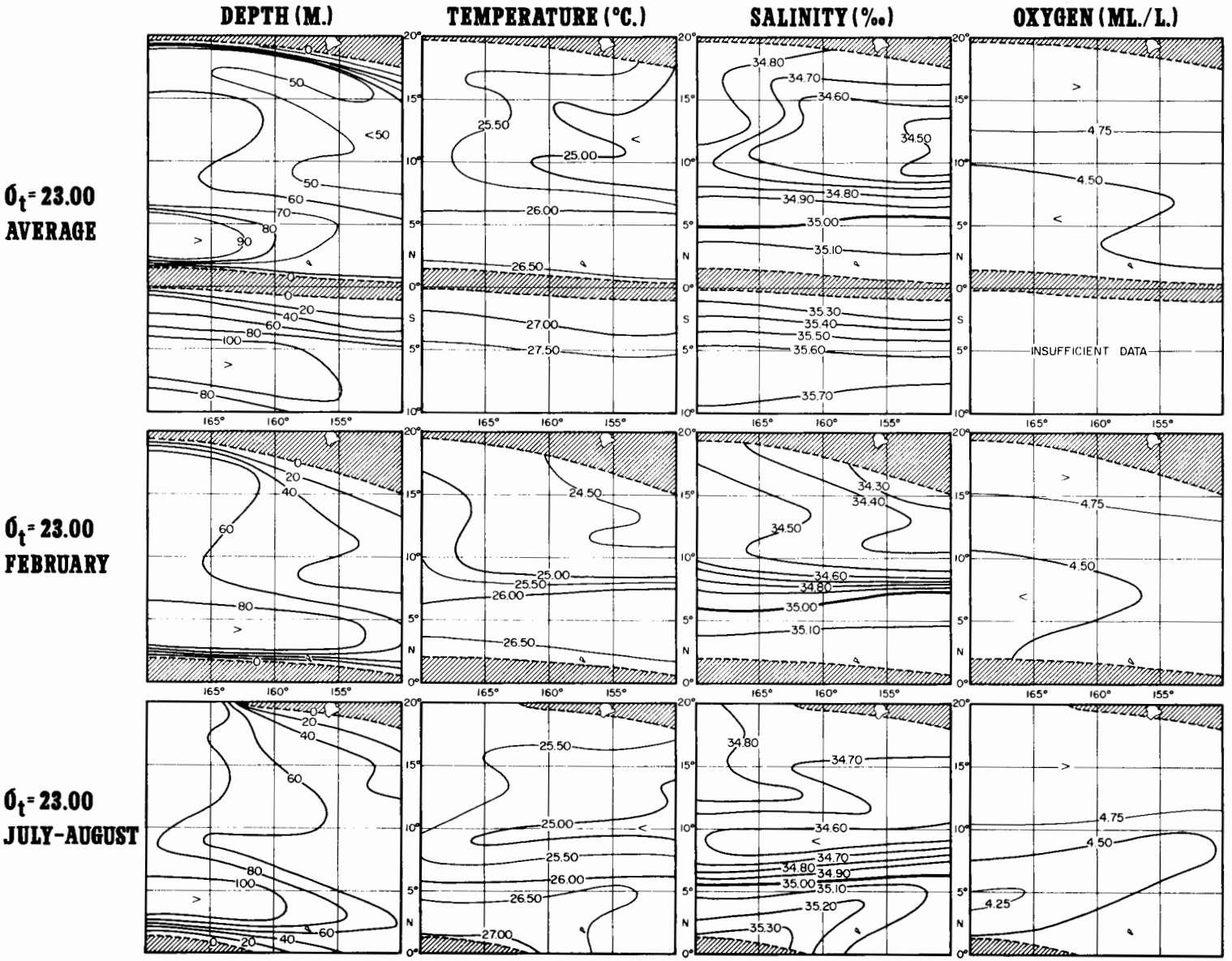

Figure 11.--Average depth and distribution of properties on a surface with a potential density of 1.0230 kg/L (σ_t = 23.00). Upper panel: Average of all values. Middle panel: February values. Lower panel: July-August values.

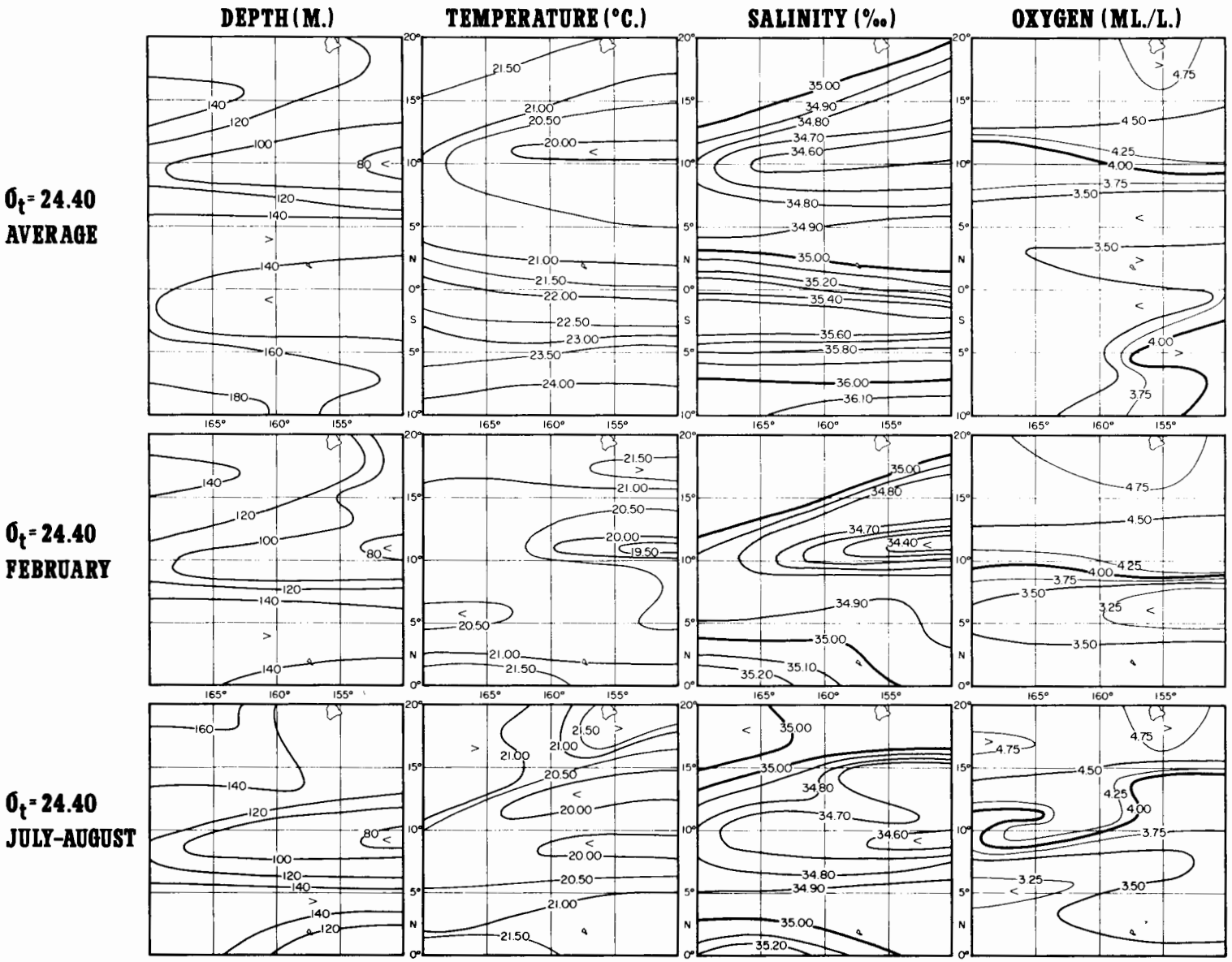

Figure 12.--Average depth and distribution of properties on a surface with a potential density of 1.0244 kg/L (σ_t = 24.40). Upper panel: Average of all values. Middel panel: February values. Lower panel: July-August values.

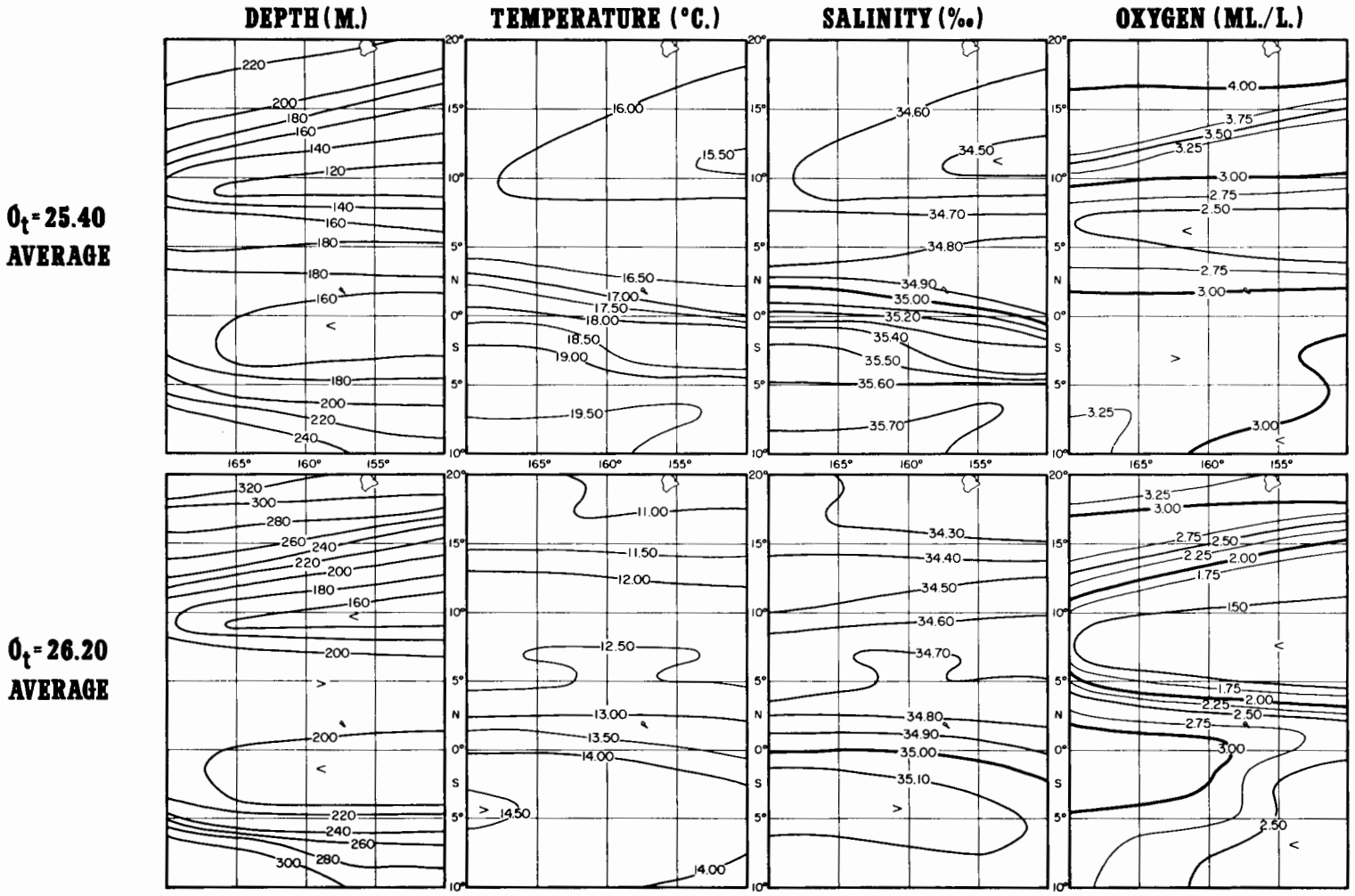

Figure 13.--Average depths and distributions of properties on surfaces with potential densities of 1.0254 and 1.0262 kg/L (σ_t = 25.40 and 26.20).

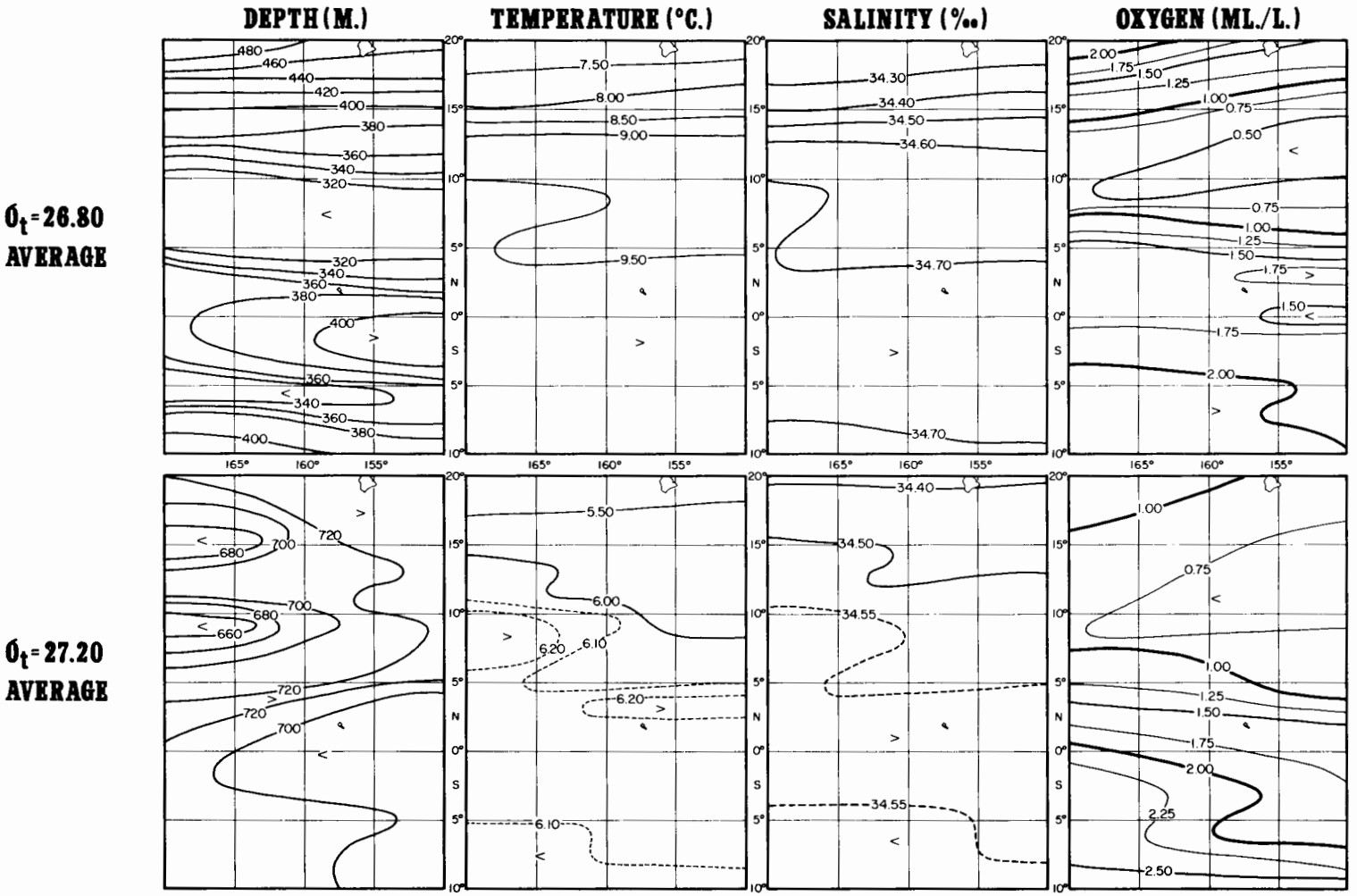

Figure 14.--Average depths and distributions of properties on surfaces of potential densities of 1.0268 and 1.0272 kg/L (σ_t = 26.80 and 27.20).

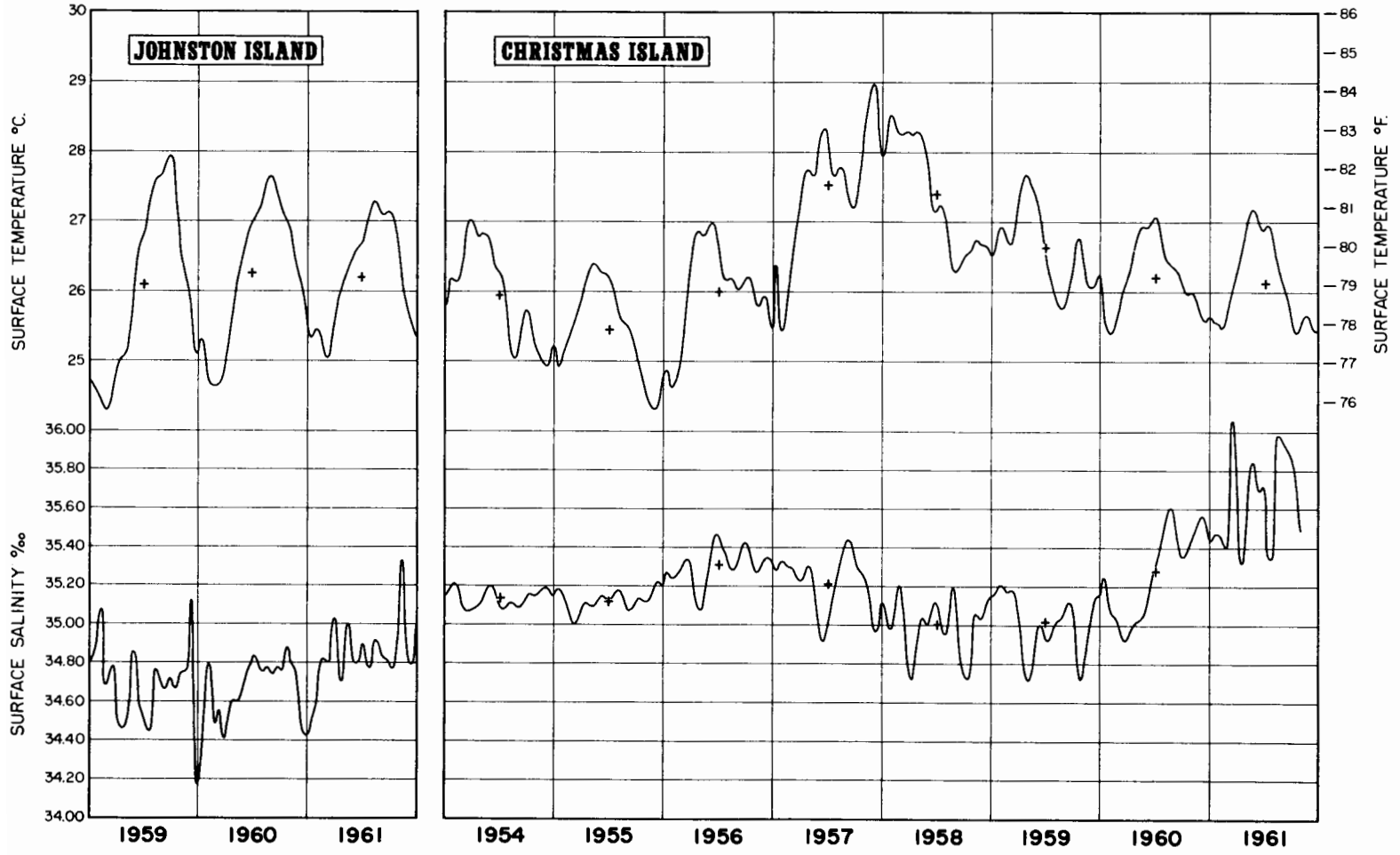

Figure 15.--Bi-monthly averages of sea surface temperatures and salinities at Johnston and Christmas Islands.